E82-10340
CR-166790
GSC-TR8203

LANDSAT-D CONICAL SCANNER EVALUATION PLAN

Prepared For

GODDARD SPACE FLIGHT CENTER

By

Stephen Bilanow

Dr. Lily C. Chen

GENERAL SOFTWARE CORPORATION

Under

Contract No. NAS5-26205

March, 1982

ABSTRACT

This document presents plans for the evaluation of the inflight performance of the Ithaco Conical Scanner onboard Landsat-D. The planned activities involved in the inflight sensor calibration and performance evaluation are discussed and the supporting software requirements are specified. It summarizes the possible sensor error sources and their effects on sensor measurements. It also presents the methods by which the inflight sensor performance will be analyzed and the sensor modeling parameters will be calibrated. In addition, a brief discussion on the data requirement for the study is provided.

TABLE OF CONTENTS

TABLE OF CONTENTS (CONT)

LIST OF ILLUSTRATIONS

LIST OF TABLES

SECTION 1 - INTRODUCTION

1.1 DOCUMENT OVERVIEW

This document presents plans for evaluation of the inflight performance of the Ithaco Conical Scanner onboard Landsat-D. This mission offers a unique opportunity to evaluate the inflight performance and accuracy of the conical scanner because accurate reference attitudes will be available from other sensors on the spacecraft, such as the star trackers. This evaluation will provide information on the attitude measurement accuracies obtainable from the newest Ithaco IR scanner design. The results will be useful for prelaunch evaluation of attitude accuracies in future missions which may use these scanners or similar scanners. The improved modeling of the Conical Scanner that results from this effort can be used in future mission support.

The Attitude Determination and Control Section (ADCS) at Goddard Space Flight Center (GSFC) has initiated this evaluation effort in order to study the inflight performance of this sensor. Originally, it was planned to evaluate the Ithaco scanner by comparing its data to the attitude solutions determined on ground using the star tracker data. However, due to the unavailability of a sufficient amount of star tracker data, the plan was altered to compare the scanner data to the attitude solutions determined from star tracker data by the onboard computer.

The primary goals of this activity are to detect the uncertainties that exist in scanner data due to localized weather effects, to determine the adequacy of the horizon radiance modeling methods, and to determine the attitude accuracies achievable using the Ithaco Conical Scanner data.

This section provides an overview of the Landsat-D mission and the conical scanner. Section 2 summarizes the planned evaluation activities, data comparison options, the modeling of the conical scanner, and the required supporting software. Sections 3 through 5 describe the basic elements of the sensor evaluation plan. Section 3 describes the sensor error sources, their effects on data, and the qualitative examination of data using data plots. Section 4 presents the inflight sensor calibration and sensor performance evaluation procedures, including the analysis of both systematic and random error sources. The data span required for the evaluation is briefly discussed in Section 5.

1.2 LANDSAT-D MISSION OVERVIEW

Landsat is a program of the Office of Space and Terrestrial Applications managed by NASA Goddard Space Flight Center. The General Electric Company Space Division is the mission contractor and is responsible for the Landsat-D spacecraft design, integration and testing, the Data Management System, the Landsat Assessment System and the Operations Control Center. The Landsat series of satellites provide multispectral imagery of the Earth's surface useful for Earth resources analysis.

Landsat-D is intended as a precursor to an operational system for global resource management. The improvements over previous Landsat spacecrafts include a higher data rate, a more accurate sensor (the thematic mapper) and a more efficient operational ground support and data management system.

The Landsat-D spacecraft design is significantly different from the previous Landsats. Landsat-D makes use of the Multimission Modular Spacecraft (MMS) design and the NASA Standard Onboard Computer (OBC) for the spacecraft control and data handling. The MMS bus includes four momentum wheels, three electromagnetic coils, and three two-axis gyroscopes for 3-axis stability, orientation and momentum control. The MMS bus also includes two NASA standard star trackers, one fine sun sensor, and a 3-axis magnetometer for attitude determination.

Landsat-D will also carry two Conical Earth sensors for Earth direction determination. The Conical Earth Sensors are built by Ithaco Inc. These sensors are used in control laws for the attitude acquisition sequence and used as backup attitude sensors by the "Safehold Electronics" to check for possible problems in the primary onboard attitude determination and control system.

Landsat-D will be launched into a circular, sun synchronous, near polar orbit with about a 708 kilometer altitude. The orbit inclination will be about 98.18 degrees with the descending node at 9:30 a.m. local time. Landsat-D is now scheduled to be launched from the Western Test Range in July 1982 onboard a Delta 3910 vehicle.

1.3 CONICAL SCANNER OVERVIEW

The conical scanner is cylindrical, 3 inches in diameter, 4 inches long, and 1.9 pounds in weight. It utilizes about 4 watts of power during operation and is designed to function at temperatures between -10^{o} and $+35^{o}$ Celsius.

A diagram of the sensor optics is shown in Figure 1-1. All of the optics (lenses, window, and prism) are made of germanium, which is nearly transparent to the infrared wavelengths detected. Infrared radiation enters the detector through a window which is coated with an interference filter. The filter/window is also coated to reflect sunlight to prevent internal heating. The filter restricts the incoming radiation to the 14 to 16 micron wavelength region. The incoming radiation is attenuated somewhat further by the other optical components. The spectral response at several stages is shown in Figure 1-2. Figure 1-3 shows the spectral bandpasses for the IR scanners on four missions for comparison. These bandpasses have been normalized to the same height to give better bandwidth comparisons. The Landsat-D scanner obviously has a narrower radiation sensitivity range.

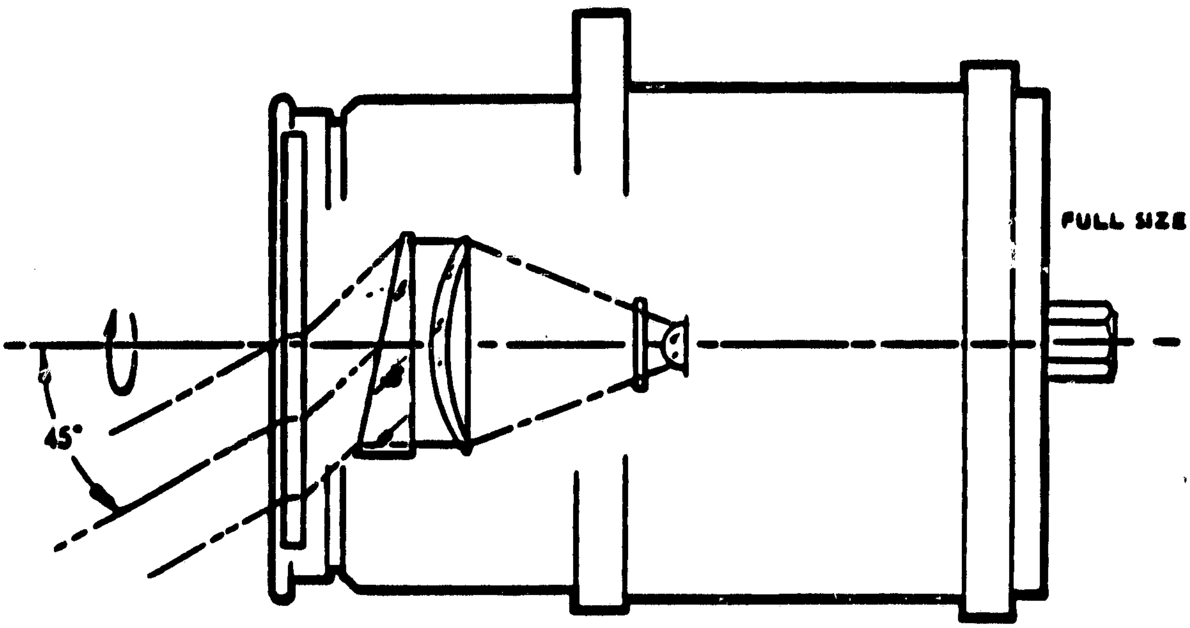

Figure 1-1 Sensor Optics Diagram (Courtesy of Ithaco Inc.)

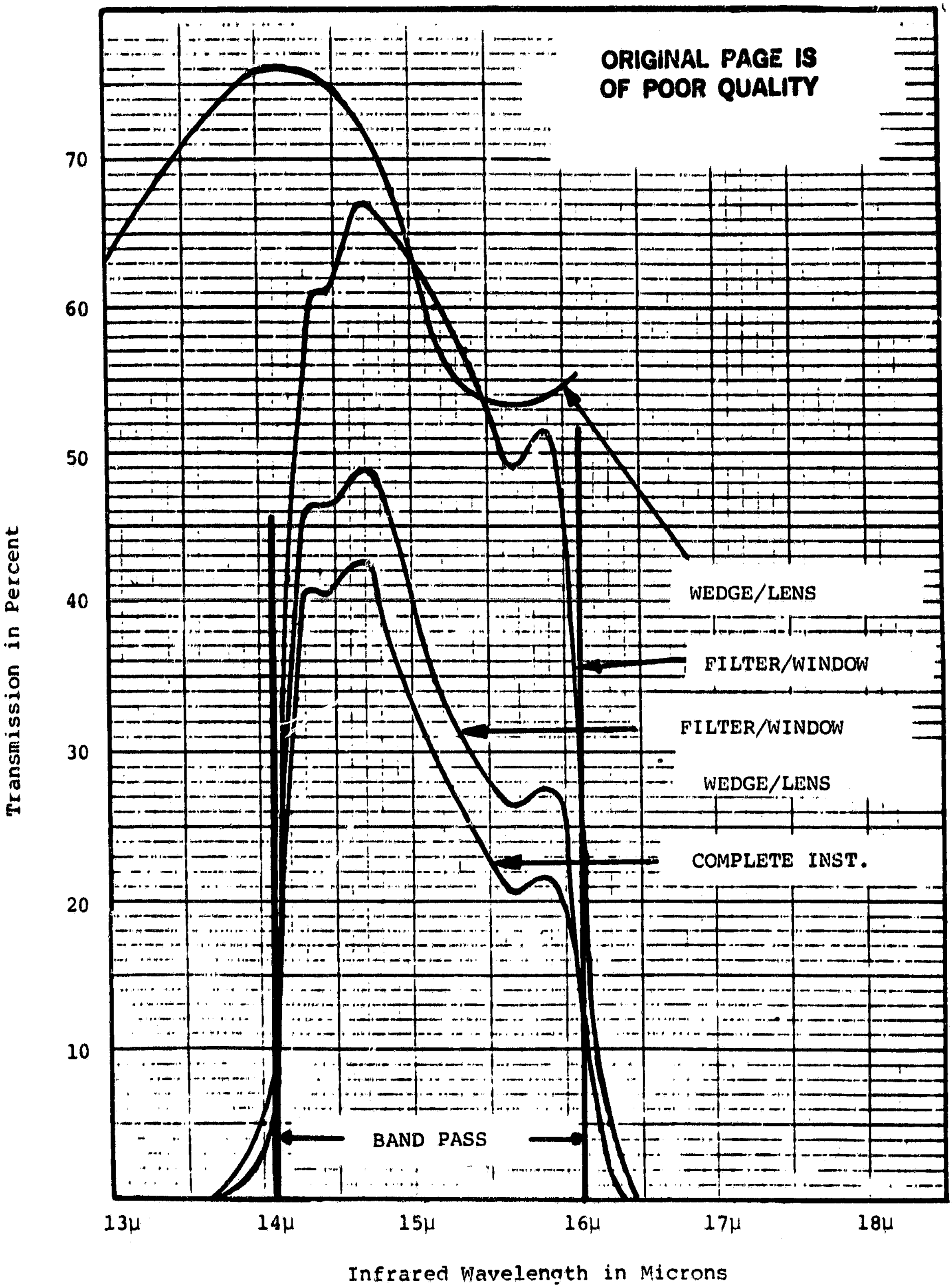

Figure 1-2 Spectral Bandpass for Landsat-D

(Courtesy of Ithaco Inc.)

ORIGINAL PAGE IS
OF POOR QUALITY

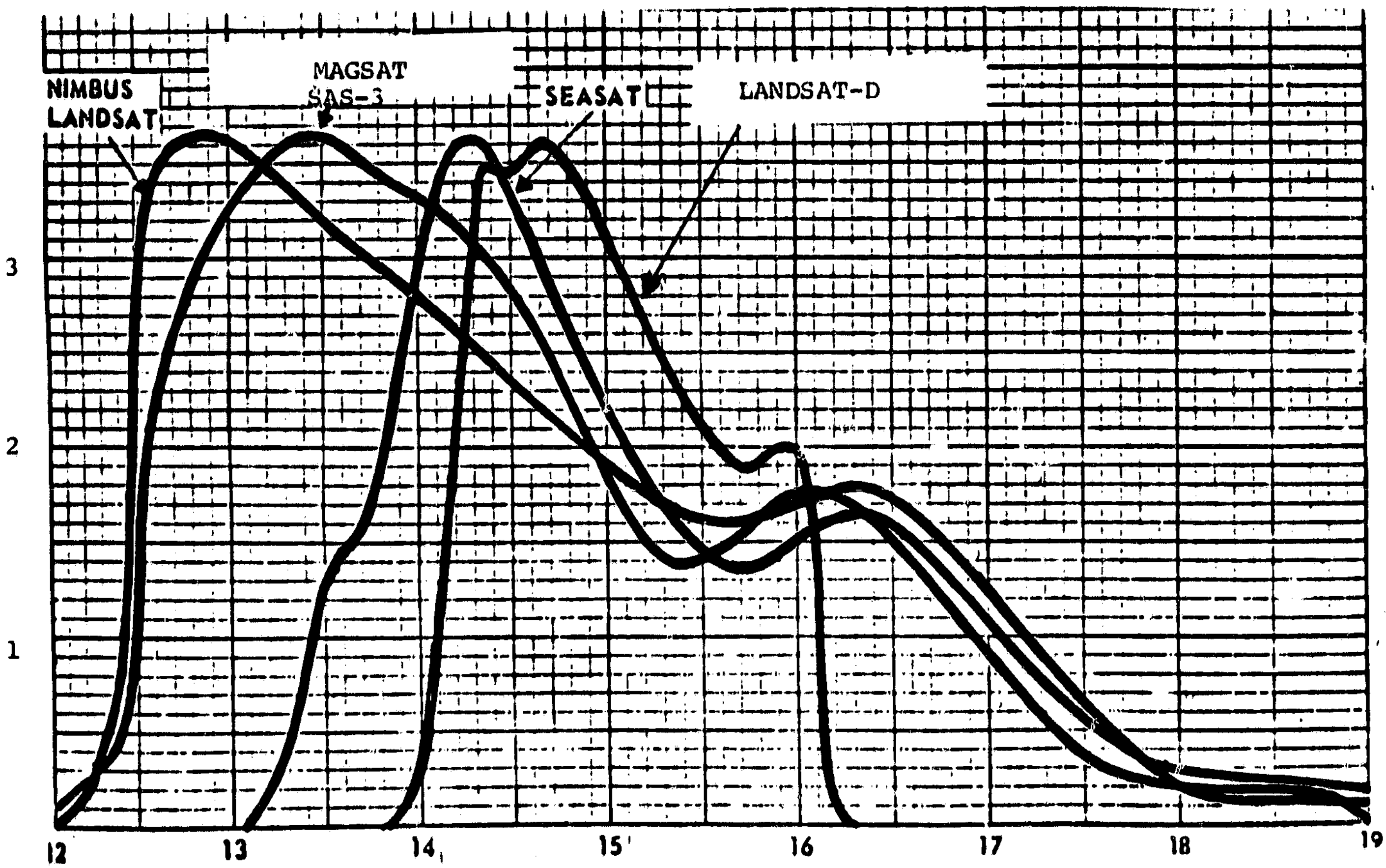

Wavelength in Microns

Figure 1-3 Comparison of Spectral Bandpasses for Four Missions. (Each curve is normalized to the same maximum height. The vertical scale has no significance)

Just inside the window/filter is a wedge or prism. The prism is designed to bend the infrared radiation along the optical axis from an angle 45 degrees off this axis. To generate the scanning motion for the bolometer field-of-view, the prism is rotated about the optical axis by a stopping motor. Thus the center of the field-of-view sweeps out a cone with a radius of 45 degrees. The scan rate or prism spin rate is 120 revolutions per minute.

After passing through the prism, incoming radiation is focused by two lenses. The bolometer is immersed in the second lens. A field stop in front of this lens acts to prevent stray radiation from entering the bolometer. All the focusing surfaces are spherical. The bolometer is placed along the optical axis in the focal plane of the lens system.

The bolometer flake is a thermistor or thermally sensitive resistor. The thermistor is a semiconductor which is made of sintered oxides of mangenese, cobalt, and nickel pressed into a thin flake. The flake measures about 0.1 millimeters square. As infrared radiation falls on the flake it is heated and its resistivity decreases. As the flake cools its resistivity increases. The time constant of the flake temperature response to radiation changes is about 2 milliseconds. The changes in current through the thermistor as the scanner field-of-view moves on and off the Earth constitute the input to the Earth Signal Processing electronics. Detailed description of the sensor electronics and the Earth signal processing is given in Reference 1. One significant difference in the conical scanner signal processing over the previous Ithaco IR scanners is the new horizon locator logic. This is shown schematically in Figure 1-4. The Earth output voltage so determined is less sensitive to the triggering levels and pulse heights of the Earth signals obtained from the bolometer.

Two horizon scanners are onboard the Landsat-D. The axis of scanner No. 1, which is called the tail-side scanner, is oriented toward the negative spacecraft velocity direction tilting 24 degrees toward the Earth center. The axis of scanner No. 2, which is called the right-side scanner, is mounted toward the negative orbit normal direction, also tilting 24 degrees toward the Earth center. The mounting geometry of the two horizon scanners in the Landsat-D spacecraft coordinate frame is shown in Figure 1-5. More detailed discussion of the Landsat-D coordinate systems and their transformations is given in Reference 1. The nominal ground tracks of

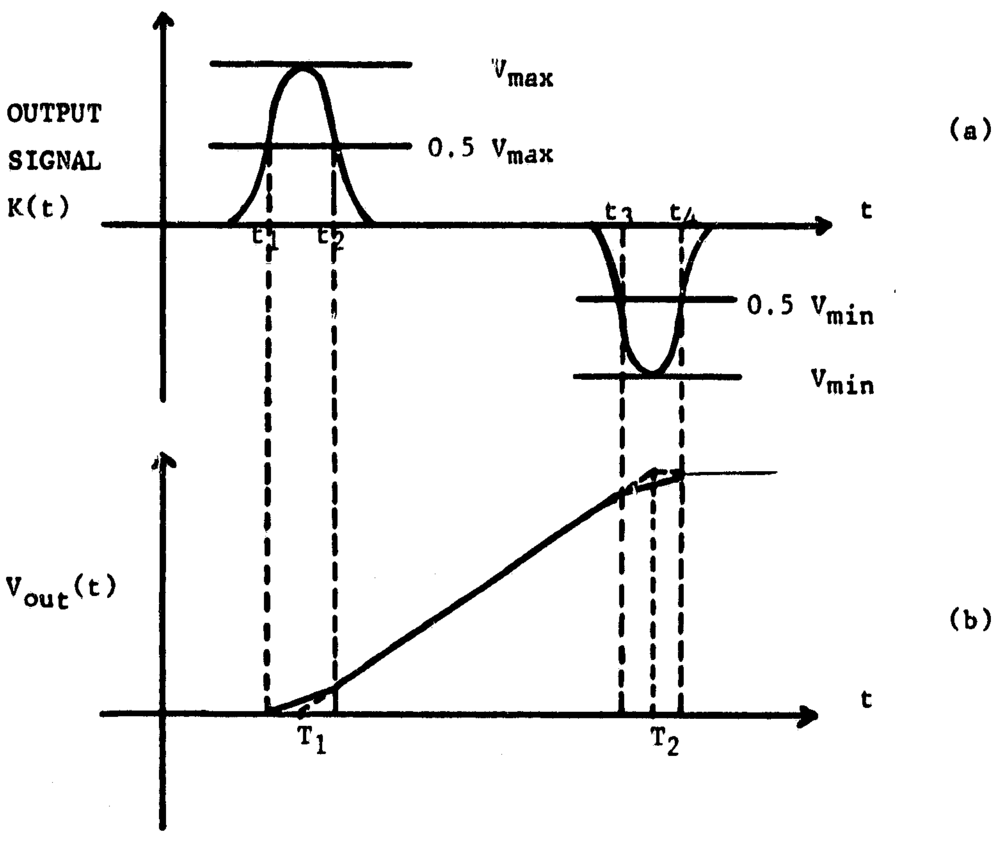

Figure 1-4 Conical Scanner E Voltage (Earth Width) Determination from the Bolometer Output Signal

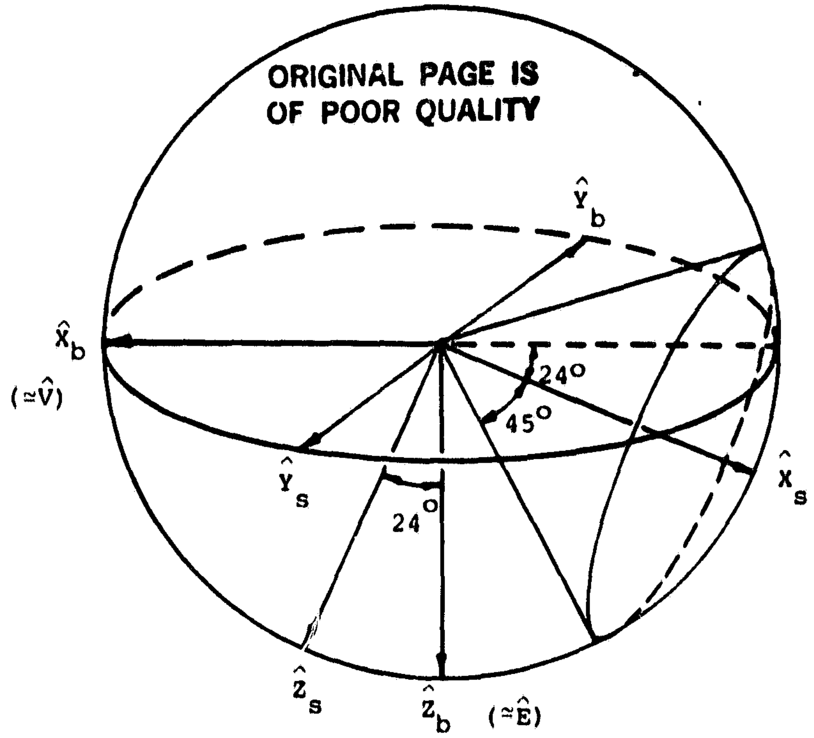

(a) Scanner No. 1 (Tail Side Scanner)

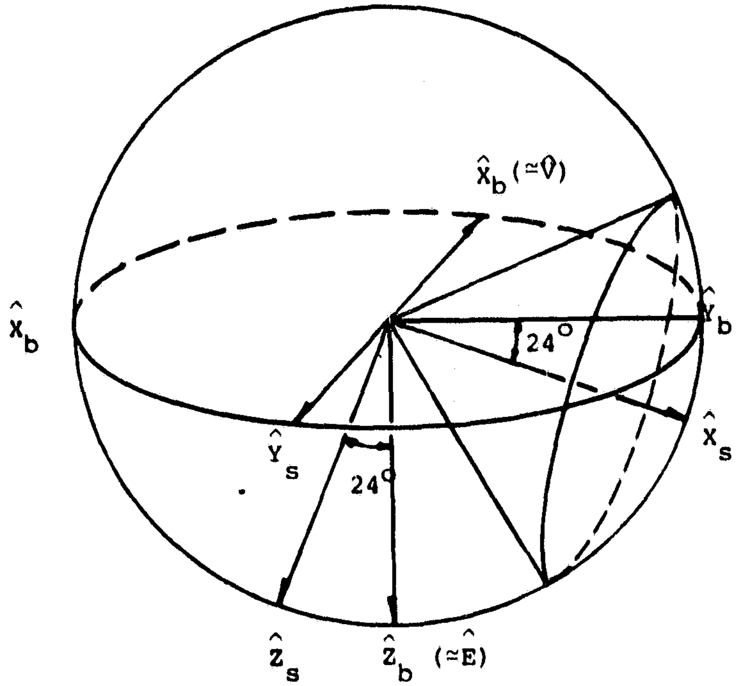

(b) Scanner No. 2 (Right Side Scanner)

Figure 1-5 Mounting Geometry of Landsat-D Concial Scanner these two scanners relative to the spacecraft flight path is shown in Figure 1-6.

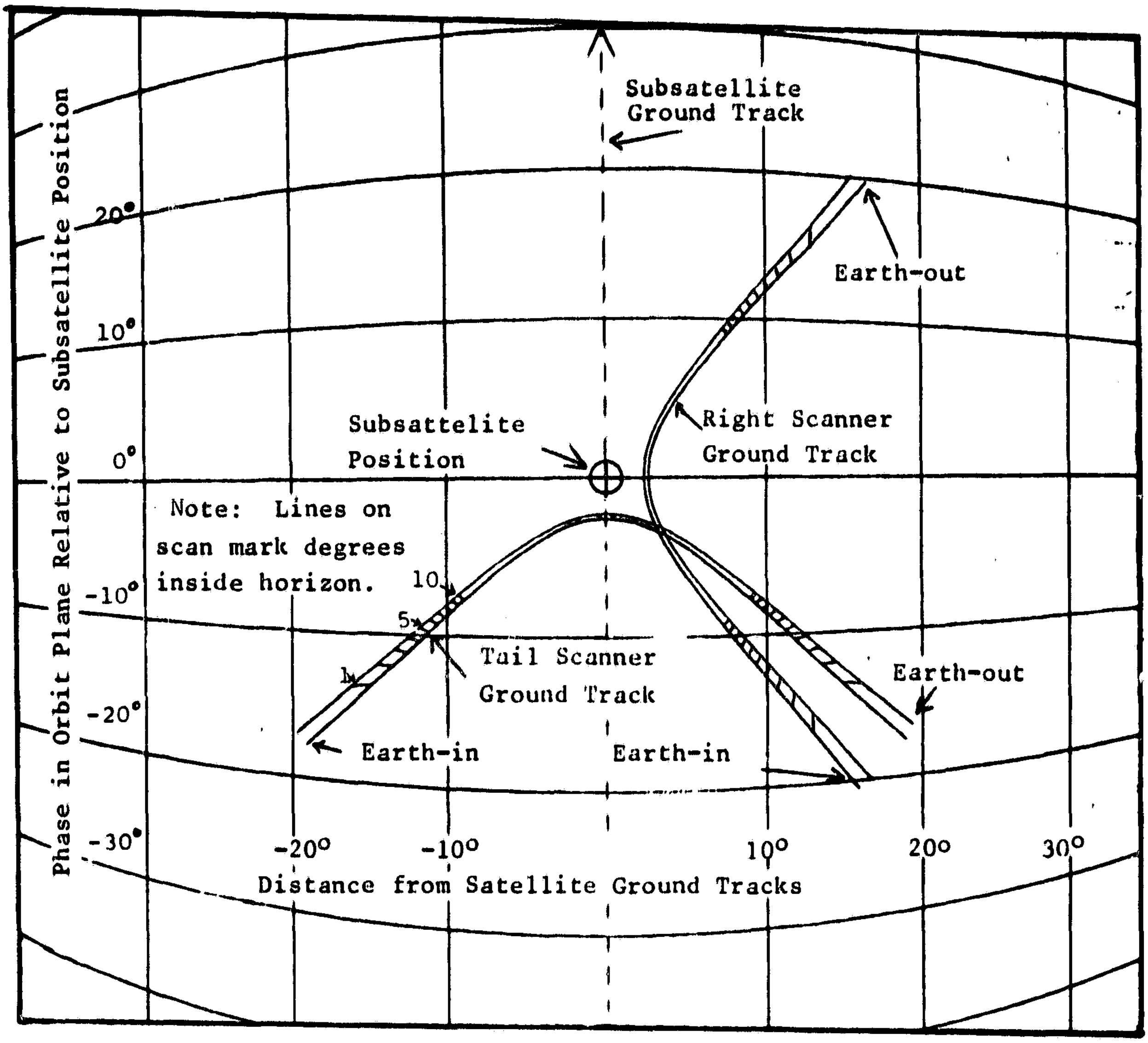

Figure 1-6 Nominal Ground Track of Conical Scanners Onboard Landsat-D.

SECTION 2 - EVALUATION PLAN OVERVIEW

2.1 PLANNED ACTIVITIES

The basic technique used in evaluating the conical scanner performance is to compare its measurements with those predicted from a reference attitude. The reference attitudes will be computed by the onboard computer (OBC) by using star tracker and gyro data. The OBC attitude solutions are expected to be accurate to better than a hundredth of a degree (Reference 2). These attitude solutions will be available in the spacecraft telemetry stream along with the conical scanner measurements.

The planned activities for Landsat-D conical scanner performance evaluation can be briefly summarized as the following:

1. Collect and process spacecraft telemetry data to retrieve horizon scanner measurements and OBC attitudes for required time spans. Store data in a data library for later evaluation purposes.

2. Predict sensor measurements using OBC attitudes and the conical scanner modeling.

3. Generate necessary data plots for qualitative comparison and review.

4. Compute residuals and statistics for quantitative error estimates.

5. Study possible error sources from residual characteristics. Differentiate systematic errors from random errors.

6. Optimize the sensor modeling parameters and determine sensor biases by minimizing the systematic residuals.

7. Study cold cloud effects and other anomalies by examining the random residuals.

8. Document results.

The following sections of this report describe these steps in more detail. This section discusses the specific data comparison options, the sensor modeling and software required to support the evaluation.

2.2 OBSERVED AND PREDICTED DATA COMPARISON

This section describes the options for comparison of the conical scanner measurements with the reference attitudes provided by the OBC.

In order to compare the scanner measurements with the reference attitude, the scanner measurements can be used to estimate the spacecraft attitude or the reference attitude can be used to estimate the scanner measurements. This is illustrated schematically in Figure 2-1, where the two basic comparison options are labeled by the dashed lines A and B.

When the measurements are converted to attitude estimates for comparison B of Figure 2-1, usually some approximations must be made. This is because a priori knowledge of the spacecraft attitude is necessary in order to make corrections for the effects of Earth oblateness and/or systematic horizon radiance variations. Since these corrections are not very sensitive to small changes in attitude, an priori estimate for the attitude (such as zero-pitch-roll-yaw for a mission like Landsat-D) is usually adequate for pitch and roll determination from the IR scanner.

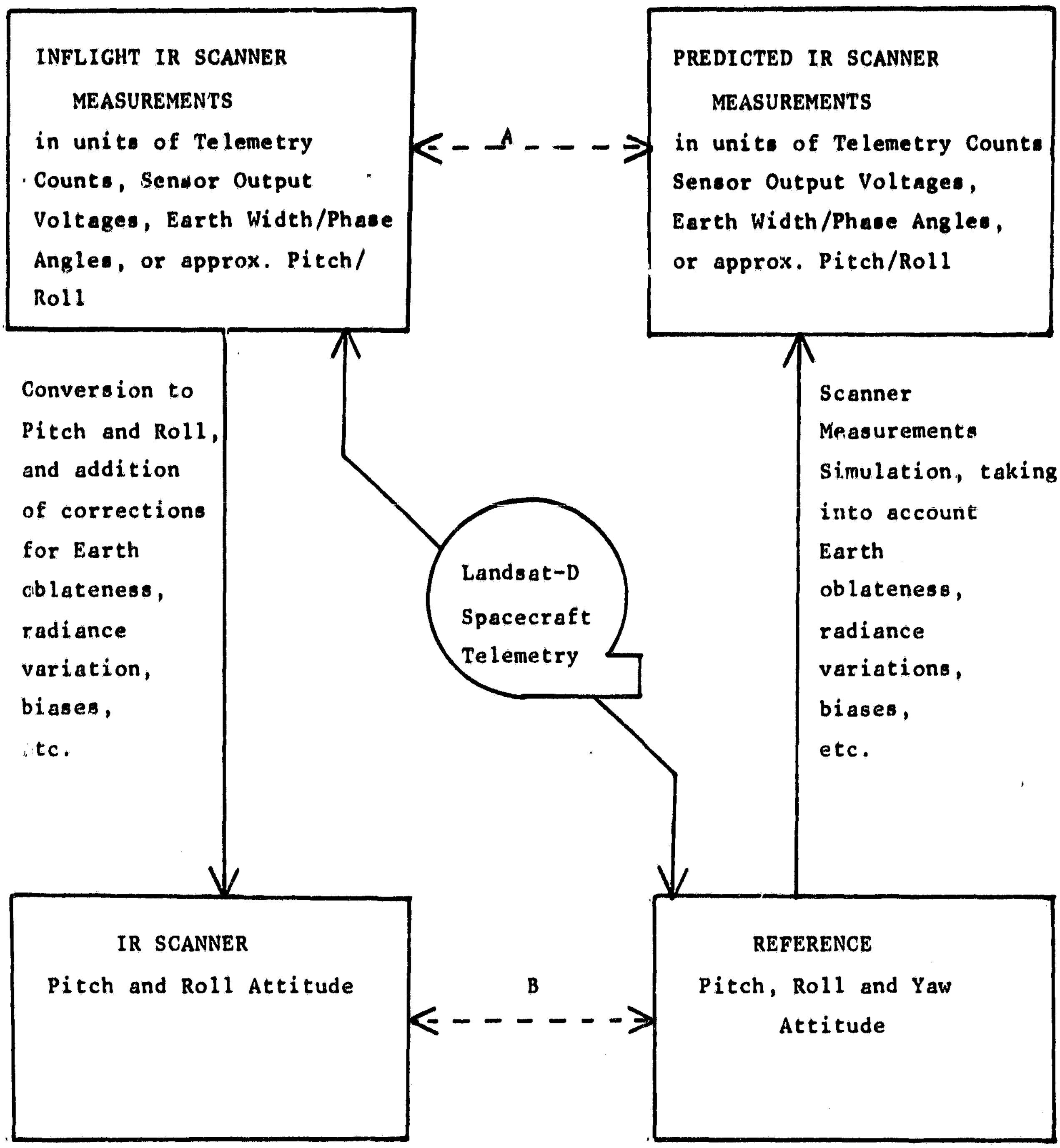

Figure 2-1 Basic IR Scanner Data and Reference Attitude Comparisons

In the case of Landsat-D IR scanner ground evaluation the available OBC reference attitude could be used to accurately correct oblateness/radiance effects. This could be done by computing the differences in the predicted measurments with and without these effects.

It is a more direct procedure to predict the conical scanner measurements from the reference attitude and make comparison A of Figure 2-1. No approximations need to be taken in this approach because the spacecraft three axis attitude is immediately available for use in the computation of Earth oblateness and horizon radiance effects. The predicted measurements can model all known features of the scanner operation. Therefore comparison A is the recommended approach for the conical scanner evaluation.

The scanner measurements may be parameterized in several ways. The most useful units are the angular measurement of Earth width Ω and phase Φ in degrees. The actual output of the scanner are voltages which are proportional to Ω and Φ. These voltages are converted to counts for the telemetry stream.

Even though the basic comparison will be made in terms of Earth width and phase angles, the residual differences in these angles can be easily converted to equivalent errors in the pitch and roll measurements. This conversion will be done by a linear relationship as a first order approximation, which is quite valid over the range of the errors.

The onboard conversion of the scanner horizon measurements to pitch and roll angles is done by assuming a linear relationship for a spherical Earth, circular orbit, and fixed conical scan. This approximation does not take into account the measurement effects due to the oblateness of the Earth, systematic horizon radiance variations, or spacecraft altitude variations. Thus the onboard pitch and roll measurements made by the horizon scanners have these error sources due to the assumptions in the computation. A more accurate IR scanner attitude is not required onboard Landsat-D.

Figure 2-2 shows in more detail the various data conversions, computations and comparisons to be made in the Landsat-D sensor evaluation. In the figure, computations are represented by solid lines, an arrow through these lines indicates that model adjustment will take place, and comparisons are represented by dashed lines. Computations for observed sensor measurements

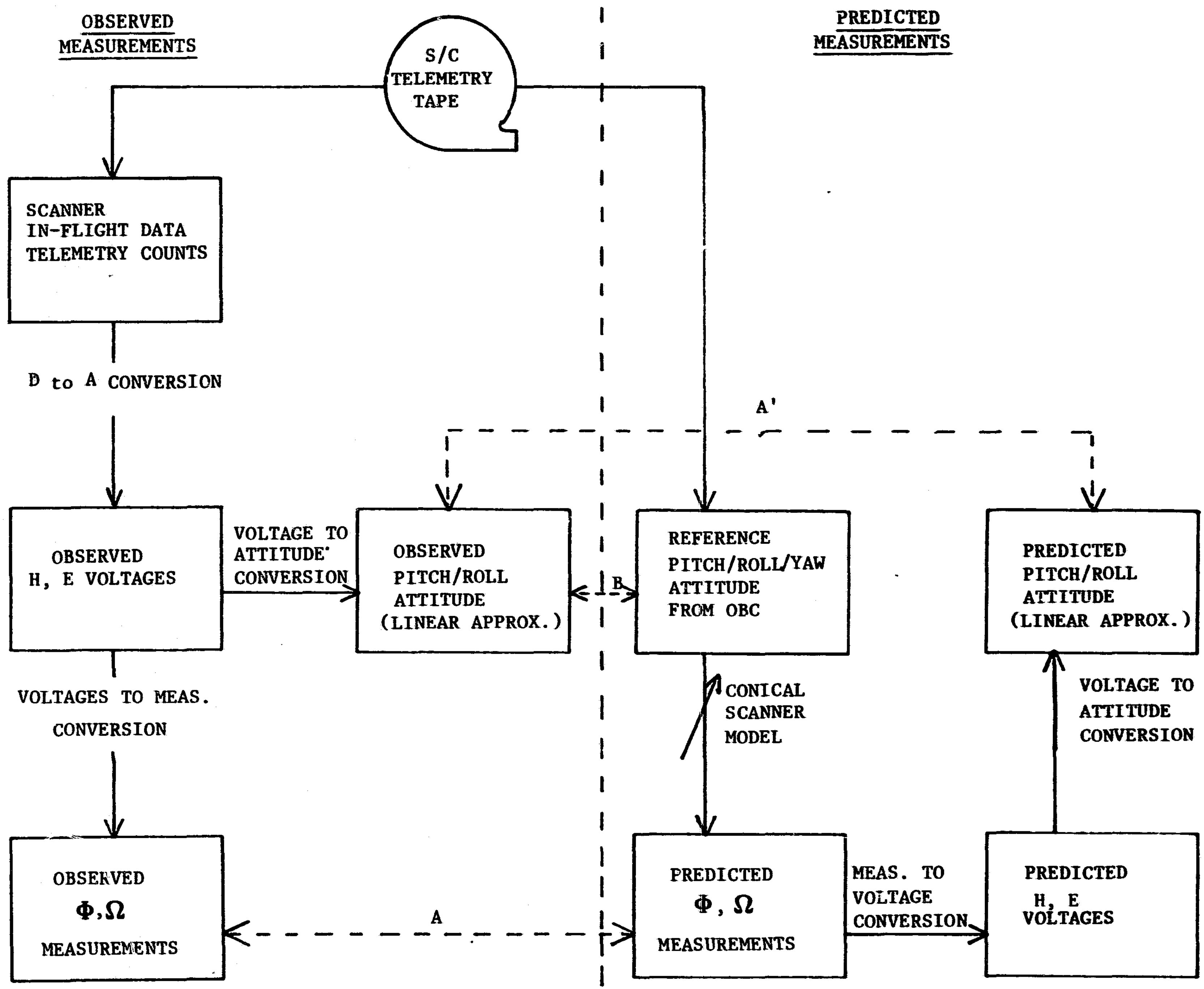

Figure 2-2 Sensor Evaluation Computations and Comparisons

are given on the left portion of the figure while those for predicted measurements are shown on the right portion of the figure. Aside from the conical scanner modeling, which involves comprehensive computations as will be discussed in Section 2.3, all other computations shown in Figure 2-2 are given by simple linear relations with specified constants.

Two comparisons are suggested as shown by the labels A (or A') and B. Note that comparison A or A' in Figure 2-2 is the same as comparison A in Figure 2-1, while comparison B of Figure 2-2 is different from that of Figure 2-1 because no corrections are made to the scanner pitch and roll estimates. The activities involved in these comparisons and their objectives are summarized below.

A. Compare the observed and the predicted conical scanner Earth measurements (in terms of Ω and Φ as in A or in terms of approximated pitch and roll as in A') to evaluate the sensor performance. Study the systematic and random error sources. Determine the sensor biases by adjusting the scanner modeling parameters to minimize the residuals.

B. Compare the attitude computed from the horizon scanner measurements through the specified linear relation used for onboard processing with the OBC reference attitude. This will show the pitch and roll measurement accuracies obtained from the conical scanner onboard the spacecraft.

As a result of these comparisons, the attitude accuracies measured by conical scanners can be determined, and the optimal sensor modeling can be obtained. Detailed descriptions for the sensor evaluation activities are given in Section 4.

2.3 CONICAL SCANNER MODELING

The mathematical modeling of the Landsat-D conical scanner is presented in detail in Reference 1. A brief summary of this modeling is given in the following.

The conical scanner is modeled in different levels of complexity in Reference 1. It starts with a simple geometrical model to determine the scanner measurements and then provides modeling for corrections due to various error sources. The simple geometrical model corresponds to an ideal situation where the sensor measurements are obtained by intersecting a conical scan with a spherical Earth under nominal conditions. The error sources considered include sensor misalignment and hardware specification errors, the Earth oblateness effects, the seasonal Earth radiance variation effects, the sensor optics and electronics responses, the sensor output voltage and telemetry calibrations, the cold cloud effects, and the random measurement noise. For some of these error sources several modeling options are described.

Due to the complexity of equations and the large amount of computations involved in the modeling of the sensor optics and electronics responses and the Earth radiance seasonal variations, this part of modeling is typically done separately to create a data base which is used to apply corrections to the geometric modeling. This type of simulation will be referred to as the sensor optics and electronics simulator (SOES) in the remainder of the document.

Thus two simulators are required to model the conical scanner measurements, one for the primary sensor measurment prediction and one for the SOES-type simulation. The computational procedure used in each of the two simulators are shown in Figures 2-3 and 2-4 respectively. The mathematical equations required in each of the computation steps are given in Reference 1.

The primary sensor measurement predictor will be used to accomplish the observed and predicted data comparison discussed in Section 2.2. The inputs to this predictor will be the reference attitudes and the measurement changes predicted by SOES due to systematic radiance variations. This predictor will include model parameters for all the following.

- Sensor mounting alignments and scan cone angle
- Geometric Earth triggering biases (triggering height and Earth angular radius)

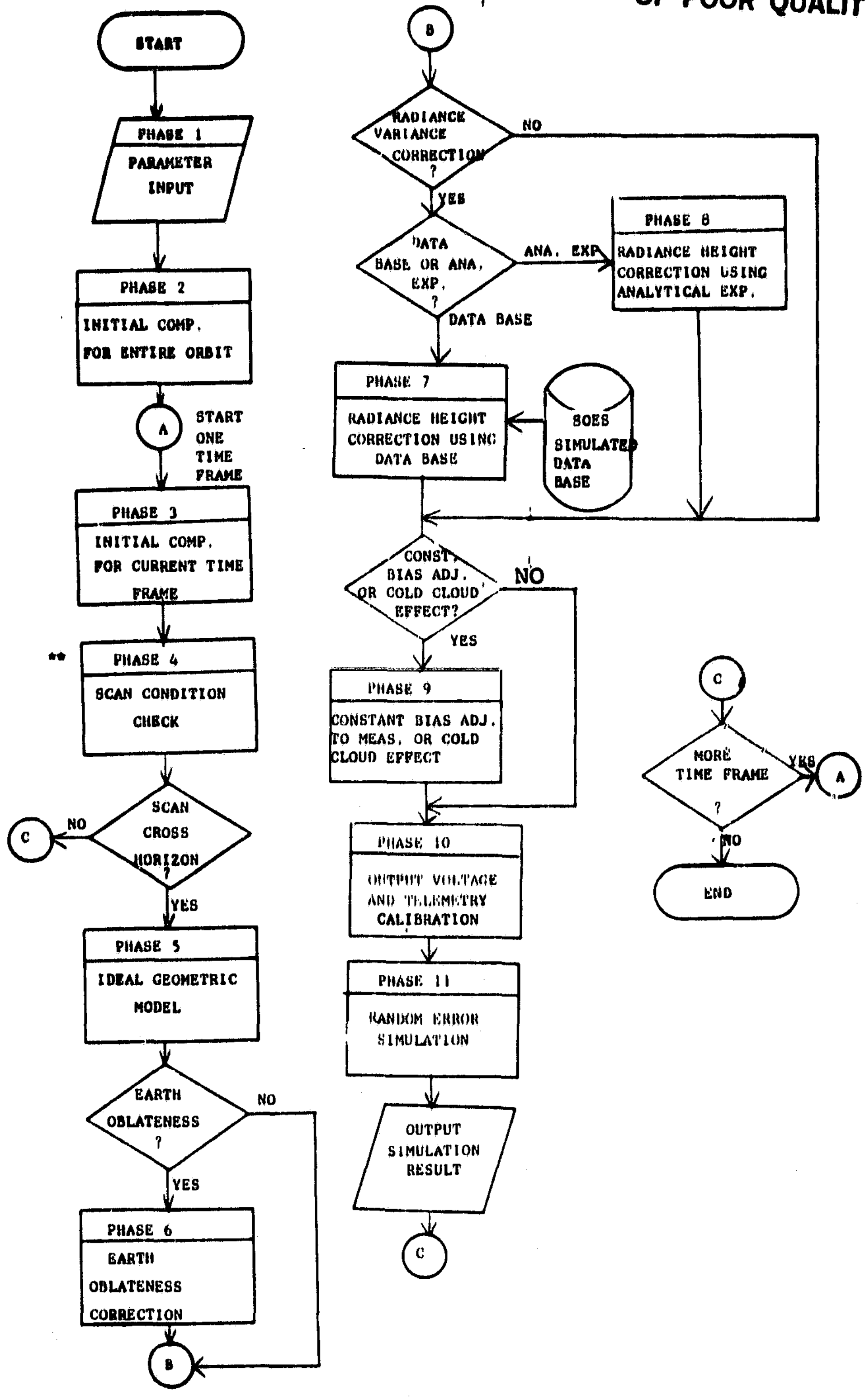

** This phase is not necessary for near nominal Landsat-D attitude.

Figure 2-3 Horizon Scanner Simulation Procedure

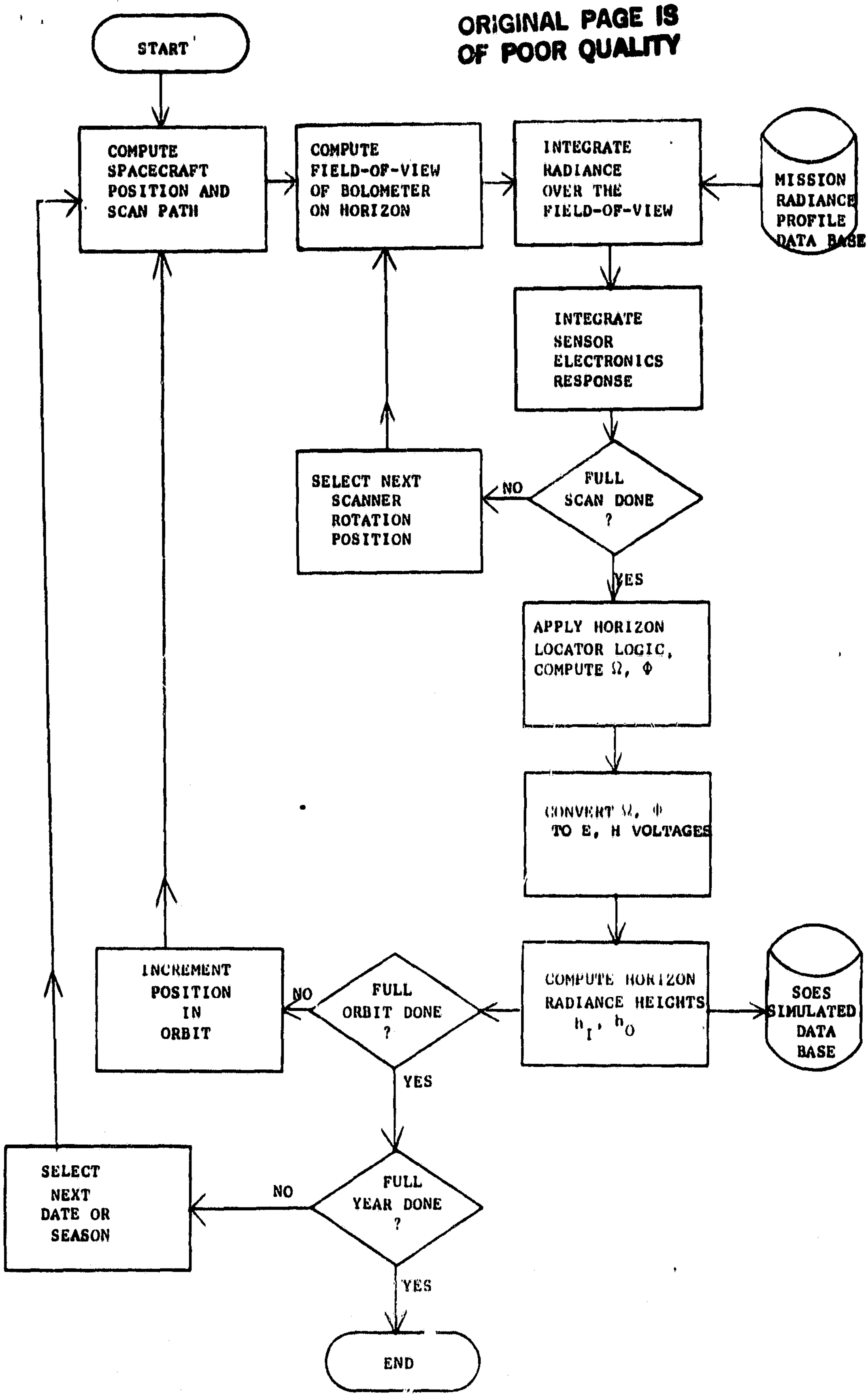

Figure 2-4 Sensor Optics and Electronics Simulation Procedure

- Constant measurement biases
- Output voltage calibrations
- A to D telemetry conversion calibrations
- Earth oblateness
- Systematic horizon radiance variation effects
- Temperature dependent errors

These model parameters will be selectively adjusted to accomplish the inflight sensor calibration.

The functional outline of the SOES-type utility is given as follows:

- Reads an input database consisting of simulated horizon radiance profiles for the Landsat-D spectral response for all latitude bands and seasons of the year.

- Integrates the simulated horizon radiance over the scanner FOV at each scan position to obtain the predicted input voltage signal from the bolometer as the scanner sweeps across the Earth.

- Convolves the bolometer input voltage signal with the signal impulse response function to obtain the predicted output signal to the horizon locator electronics.

- Applies the horizon locator logic to the sensor electronics output signal to obtain the direction of the center of the sensor FOV at the horizon triggering time. This is expressed as an effective altitude or tangent height of the center of the sensor FOV above the surface of the Earth at the time of triggering.

- Obtains predicted horizon triggering heights for each scanner horizon crossing for each orbit position and season of the year.

Some more discussion of these two simulators and their interface with other utilities is given in Section 2.4.

2.4 SOFTWARE REQUIREMENTS

The conical scanner evaluation activities described in this report require a system to execute the nine utility functions as summarized in Table 2-1. The data flow between the various functions is shown in Figure 2-5. A brief description of the utility functions and their interfaces follows. These utilities can be designed as independent programs interfacing through the datasets, or some of the functions may be combined in one program. These utility programs will be developed to run in batch mode on the IBM 360/95 or 360/75 computer. The details of these programs will be worked out in the upcoming software design effort and will be available in June, 1982.

Telemetry Processor

The function of the Telemetry Processor is to extract the necessary attitude data from the spacecraft telemetry and store it in another much smaller dataset. The spacecraft telemetry stream contains a large volume of science and engineering data of which only a small part relates to the attitude measurments. The telemetry data words which relate to the Earth Sensor Assemblies are shown in Figure 2-6 (Reference 3). In addition to

TABLE 2-1 Utility Software Functions

1. Telemetry Processor
2. Spectral Bandpass Integration
3. Sensor Optics and Electronics Simulator
4. Scanner Measurement Predictor
5. Data Plotter
6. Residual Statistics
7. Polynomial Fits
8. Finite Fourier Series Fits
9. Scan Path Plotter

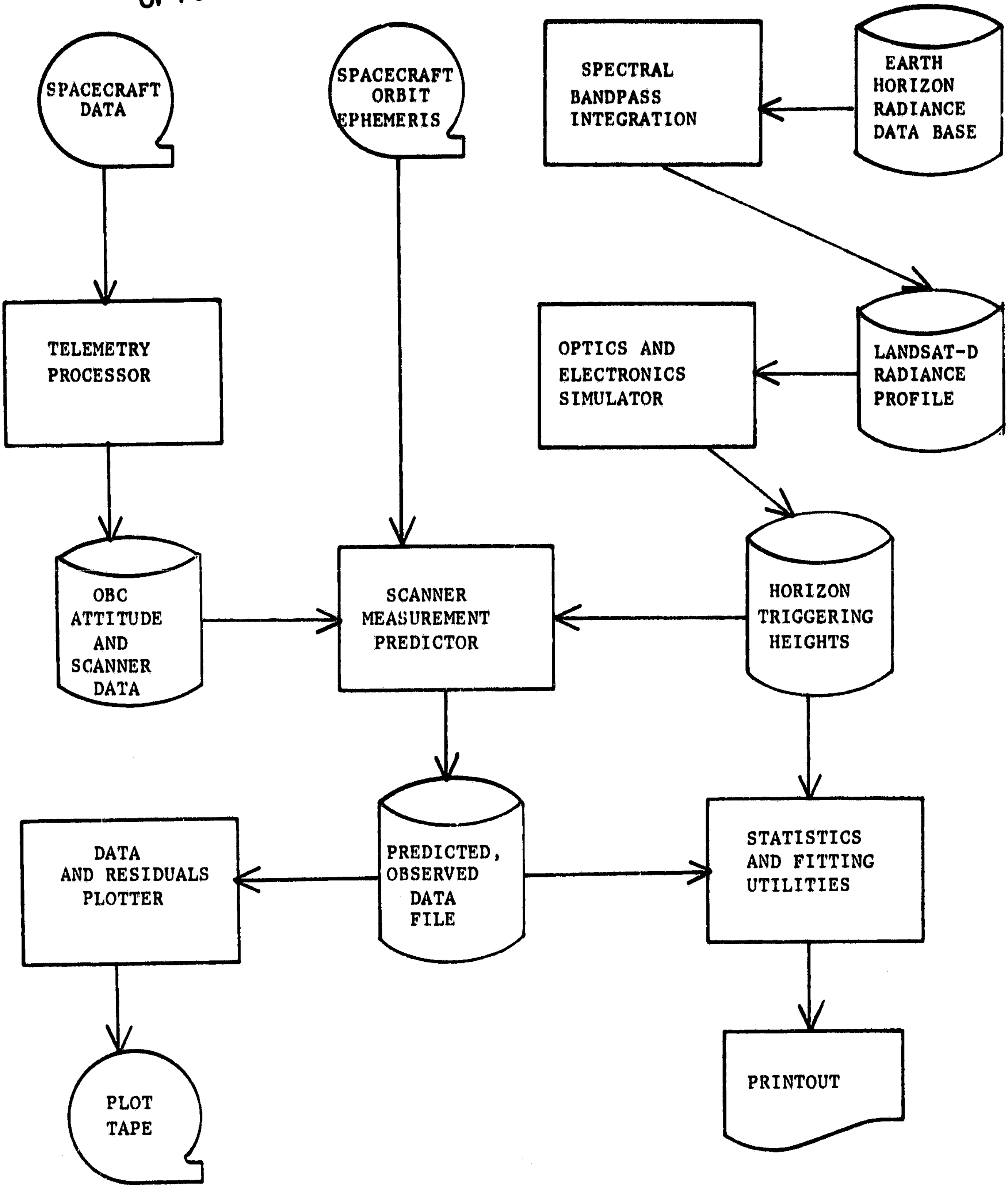

Figure 2-5 Conical Scanner Evaluation System Data Interfaces

47J249-UDAR REV. LANDSAT D ELECTRICAL SYSTEM SCHEMATIC, TELEMETRY LIST

USER ID	TLM FUNCTION DESCRIPTION	SGNL TYPE	MTX LOC COL,ROW	SMPL RATE	M	ADDRESS RIU-CH	RIU CONN	S/S CONN	I/F CONN
ESAM-01	ESA-1 PITCH FINE ERROR	ALOG	8	128		04-48			
ESAM-05	ESA-2 PITCH FINE ERROR	ALOG	9	128		04-52			
ESAM-02	ESA-1 PITCH COARSE ERROR	ALOG	40	128		04-49			
ESAM-06	ESA-2 PITCH COARSE ERROR	ALOG	41	128		04-53			
ESAM-03	ESA-1 ROLL FINE ERROR	ALOG	72	128		04-50			
ESAM-07	ESA-2 ROLL FINE ERROR	ALOG	73	128		04-54			
ESAM-04	ESA-1 ROLL COARSE ERROR	ALOG	104	128		04-51			
ESAM-08	ESA-2 ROLL COARSE ERROR	ALOG	105	128		04-55			
ESAM-09	ESA-1 SIGNAL STATUS	ALOG	38	128		04-59			
ESAM-10	ESA-2 SIGNAL STATUS	ALOG	102	128		04-62			
ESAM-11	ESA-1 SENSOR STATUS	ALOG	99,06	4		04-57			
ESAM-12	ESA-2 SENSOR STATUS	ALOG	99,22	4		04-58			
ESAM-13	ESA-1 TEMPERATURE	ALOG	33,44	1		04-56			
ESAM-14	ESA-2 TEMPERATURE	ALOG	33,46	1		04-63			
ESAM-15	ESA-1 BOLOMETER TEMPERATURE	ALOG	33,47	1		04-60			
ESAM-16	ESA-2 BOLOMETER TEMPERATURE	ALOG	33,48	1		04-61			

ORIGINAL PAGE IS OF POOR QUALITY

Figure 2-6 Earth Sensor Assemblies 1 and 2 Telemetry Words this data, the telemetry processor must extract the associated GMT times, and the OBC attitude solutions. The OBC attitude is provided every four seconds.

Spectral Bandpass Integration

A Horizon Radiance Data Base (HRDB) is being prepared to describe the Earth infrared radiance in a mission independent format. This data base will contain average Earth radiance profiles for each latitude band and season and a range of small spectral intervals around 14 to 16 microns. These radiance profiles will be derived from an Air Force Earth radiance model, LOWTRAN V (Reference 4).

This utility will extract the radiance profiles from the HRDB and integrate the radiances over the specific spectral bandpass of the Landsat-D conical scanners to obtain a set of radiance profiles for the Landsat-D mission analysis. These Landsat-D radiance profiles will be used as input to the sensor optics and electronics simulator.

Sensor Optics and Electronics Simulator

The main function of the sensor optics and electronics simulator (SOES) will be to predict the sensor response to seasonal, systematic, Earth radiance variations. The computational procedure of SOES is shown in Figure 2-4 and discussed in Section 2.3. It will read a radiance profile data base and output a horizon triggering heights data base. The SOES can also be used as an analytical tool to study the sensitivity of the scanner measurements to various detailed model parameters.

Scanner Measurement Predictor

The main functions of the measurement predictor will be to compute the predicted sensor measurement based on the OBC attitude and generate a file with the predicted and observed measurements for the generation of data plots and analysis by the statistics and fitting utilities. The measurement predictor will include a comprehensive model of the conical scanner and Earth, with all significant error sources for the scanner modeled. The computational procedure of this predictor is shown in Figure 2-3. The adjustment of the scanner measurement predictor model parameters will form the basis for the inflight calibration of the sensor. The output to the plot file will include, in addition to the predicted and observed measurements, all parameters which might conceivably be useful for correlation with the measurement errors. A list of parameters needed to be included in the plot file is given in Table 2-2. The signal status and sensor status words will not normally be examined, but they are included in the plot file so that they can be easily checked if data anomolies appear in the plots.

The scanner measurement predictor can also be very useful as an analytical tool for studying the error sources. In order to make it particularly useful as an analytical tool, options will be included to

1) input an attitude from some other source than the OBC telemetry (e.g. constant p,r,y or tabular attitude history), and

2) simulate ideal measurements in place of the observed data normally written to the plot file.

In this way predicted measurements can be simulated for two sets of model parameters and the differences can be plotted with the plot utility and analyzed with the statistics utilities. This will make the testing of the effects of model variations very convenient.

Data Plotter

The plot utility will provide Calcomp plots with general scaling options of any of the parameters included on the

TABLE 2-2 Plot File Parameters

	Notes
Observed Scanner Measurements	
Earth width	1, 2
Earth phase	1, 2
Earth-in angle	1, 2, 3
Earth-out angle	1, 2, 3
Predicted Scanner Measurements	
Earth width	1
Earth phase	1
Earth-in angle	1, 3
Earth-out angle	1, 3
Resdual Errors	
Earth width	1
Earth phase	1
Earth-in angle	1, 3
Earth-out angle	1, 3
Pitch error	1, 3
Roll error	1, 3
Earth-in triggering heights	1, 3
Earth-out triggering heights	1, 3
Bolometer Temperature	1
Scanner Assembly Temperature	1
Signal Status	1
Sensor Status	1
Predicted Horizon Crossing Latitudes	
Earth-in	1
Earth-out	1
Reference Attitude	
Pitch	
Roll	
Yaw	

TABLE 2-2 Plot File Parameters (cont)

Spacecraft Altitude

Subsatellite Latitude

Subsatellite Longitude

Satellite orbit phase angle relative to the ascending node

Notes

1. Measurement taken for each scanner separately.

2. Nominally, the fine measurements are used and the course measurements are dropped.

3. Can be derived from Ω, Φ, Ω_p, Φ_p by a simple relationship and therefore need not actually be stored on the plot file.

plot file (which is output by the measurement predictor). The most commonly used option will be the plotting of the measurements vs. time, but any of the variables in the file could be plotted against the other. Plots of several parameters can be overlaid on the same graph or stacked on top of each other. This flexibility will allow the generation of plots of a large number of important parameters, and allow visual correlation of one variable with another.

Residuals Statistics

The data statistics utility will serve the simple function of generating mean and standard deviation statistics on the measurements and residuals. The input file to the statistics utility is the same file as the input to the plot generator.

Polynomial Fit

The polynomial fit utility also performs a simple computational function that could be accomplished by reading the plot file. Some existing polynomial fit subroutines recieve data from an array. However in this case, because of the long data spans, it is practical to read the data file sequentially and compute the fit.

Finite Fourier Series Fit

The finite Fourier series fit is another computational function that could be accomplished by reading the plot file. It can also be used to fit the horizon triggering height data base to provide parameters for an analytical representation of the data base.

Scan Path Plotter

A utility program was developed and used for Seasat and Magsat mission analyses to plot the path of the scanner field of view across the Earth's surface. This utility is useful for a general understanding of the scan geometry, and particularly useful for showing the scan path on the Earth when the measurements are impacted by cold clouds. The scan path plots can be overlaid on GOES Earth photographs.

The existing utility will be modified so that the spacecraft attitude and orbit parameters can be input in a convenient, user oriented format for Landsat-D.

SECTION 3 - ANALYSIS OF ERRORS

3.1 ERROR SOURCES

The principal error sources for the Landsat-D conical scanner and their effects on the sensor measurments are shown in Table 3-1. Here an error source is defined as an effect which can make the horizon scanner measurements different from those predicted by a simple geometrical model. A brief discussion of these error sources follows, along with some discussion of the past mission experience with these errors and their relevance to Landsat-D. The utility programs discussed in the previous section will serve as analysis tools for the detailed modeling of these error sources for the inflight evaluation.

3.1.1 Constant Biases

For the Landsat-D nominal attitude and orbit, i.e., zero pitch, roll, yaw and circular orbit, biases in many of the sensor model parameters have a virtually constant effect on the Earth measurements. Thus it is logical to solve for constant biases in the measurements which will effectively adjust for the sum effect of all the correlated bias parameters. This is the approach taken

ORIGINAL PAGE IS
OF POOR QUALITY

TABLE 3-1 ERROR SOURCES FOR LANDSAT-D CONICAL SCANNER AND THEIR EFFECTS ON THE SENSOR MEASUREMENTS

<table>
<tr><th rowspan="3">ERROR CATEGORY</th><th rowspan="3">DESCRIPTION</th><th rowspan="3" colspan="2">ERROR SOURCES</th><th colspan="4">EFFECTS ON CONICAL SCANNER PITCH/ROLL MEASUREMENTS*</th></tr>
<tr><th colspan="2">SENSOR 1</th><th colspan="2">SENSOR 2</th></tr>
<tr><th>PITCH ERROR</th><th>ROLL ERROR</th><th>PITCH ERROR</th><th>ROLL ERROR</th></tr>
<tr><td rowspan="12">1</td><td rowspan="12">Errors that give nearly constant effect on sensor measurements.</td><td rowspan="6">Earth Width Correlated Errors</td><td>Earth width bias</td><td rowspan="6">Constant</td><td rowspan="6">--------</td><td rowspan="6">--------</td><td rowspan="6">Constant</td></tr>
<tr><td>E-voltage offset</td></tr>
<tr><td>Triggering height bias</td></tr>
<tr><td>Earth Angular radius bias</td></tr>
<tr><td>Scan cone angle bias</td></tr>
<tr><td>Scanner tilt misalignment</td></tr>
<tr><td rowspan="4">Earth Phase Correlated Errors</td><td>Earth Phase bias</td><td rowspan="4">--------</td><td rowspan="4">Constant</td><td rowspan="4">Constant</td><td rowspan="4">--------</td></tr>
<tr><td>H-voltage offset</td></tr>
<tr><td>Reference pulse time delay</td></tr>
<tr><td>Scanner twist misalignment</td></tr>
<tr><td colspan="2">Pitch offset bias</td><td>Constant</td><td>--------</td><td>Constant</td><td>--------</td></tr>
<tr><td colspan="2">Roll offset bias</td><td>--------</td><td>Constant</td><td>--------</td><td>Constant</td></tr>
<tr><td rowspan="3">2</td><td rowspan="3">Errors that give nearly orbital frequency effects on sensor measurements</td><td colspan="2">Spacecraft Altitude</td><td>Orbit frequency</td><td>--------</td><td>--------</td><td>Orbit frequency</td></tr>
<tr><td colspan="2">Earth Oblateness</td><td>Twice orbit frequency</td><td>--------</td><td>Twice orbit frequency</td><td>Twice orbit frequency</td></tr>
<tr><td colspan="2">Seasonal systematic horizon radiance variations</td><td>Orbital frequency</td><td>--------</td><td>Orbital frequency</td><td>Orbital frequency</td></tr>
<tr><td rowspan="4">3</td><td rowspan="4">Errors that have dependence on specific variables</td><td rowspan="2">Temperature Dependent Errors</td><td>Changes in pre-amplifier gains</td><td>Bolometer temp. dependent</td><td>Bolometer temp. dependent</td><td>Bolometer temp. depend.</td><td>Bolometer temp. dependent</td></tr>
<tr><td>Changes in scan rate and other electronic responses.</td><td>Sensor elect. temp. depend.</td><td>Sensor elect. temp. depend.</td><td>Sensor elect. temp. depend.</td><td>Sensor elect. temp. depend.</td></tr>
<tr><td rowspan="2">Earth Width or Phase Dependent Errors</td><td>E-voltage calibration error</td><td>Earth-width or pitch depend.</td><td>--------</td><td>--------</td><td>Earth-width or roll depend.</td></tr>
<tr><td>H-voltage calibration error</td><td>--------</td><td>Earth-phase or roll dependent</td><td>Earth-phase or pitch dependent</td><td>--------</td></tr>
<tr><td rowspan="2">4</td><td rowspan="2">Errors that have random effects on sensor measurements</td><td colspan="2">Electronic noise</td><td>High frequency random</td><td>High frequency random</td><td>High frequency random</td><td>High frequency random</td></tr>
<tr><td colspan="2">Random horizon radiance variations due to cold clouds</td><td>Low frequency random</td><td>Low frequency random</td><td>Low frequency random</td><td>Low frequency random</td></tr>
</table>

* "--------" indicates that the corresponding error is either zero or non-significant under nominal Landsat-D geometry.

in previous similar missions. It is also the approach taken implicitly by Ithaco in their ground calibration of the scanner via the bench test. The detailed measurement predictor can be used as a tool to show what extent the model parameters have any non-constant effect on the measurements over each orbit at the actual flight attitude. Only parameters with a significant non-constant effect can be distinguished from the constant measurement bias effects.

In the Magsat mission inflight data analysis a constant pitch bias was found to be stable from orbit to orbit, but the bias value gradually changed by about 0.2 degrees over 5 months of the mission (Reference 6). It is therefore very important to check the biases stability over a long time span.

3.1.2 Orbital Period Effects

Earth oblateness has a double orbital frequency effect on the measurements, while systematic horizon radiance variations have both orbital and double orbital components that vary with the season. The Earth oblateness is well modeled, and it is not a significant error source unless ignored for simplicity as in the onboard scanner pitch, roll determination. For Landsat-D, the magnitude ranges of the corrections to the pitch and roll measurements due to the effects of Earth oblateness are as follows: For the scanner 1 pitch and acanner 2 roll, it is $\pm$ 0.25° with maximum corrections near equator and pole crossings. For the scanner 2 pitch measurement it is $\pm$ 0.17°, with maximum corrections near the $\pm$ 45° latitudes. For the scanner 1 roll measurement the oblateness correction is insignificant, $\pm$ 0.05°, because both horizons view similar latitudes.

The Earth horizon radiance variations and their effects on the sensor measurements are more difficult to model. The SOES utility is specifically designed to predict these effects, taking into account the sensor field-of-view and electronics responses. The SOES utility will be used to generate plots of the Landsat-D predicted horizon radiance effects as a function of orbit position and horizon crossing latitude. A sample plot of the predicted effects of the systematic horizon radiance variations on the Magsat IR scanner measurements as a function of orbit position is given in Figure 3-1. It is a major goal of the Landsat-D conical scanner evaluation to test the adequacy of the current systematic horizon

ORIGINAL PAGE IS
OF POOR QUALITY

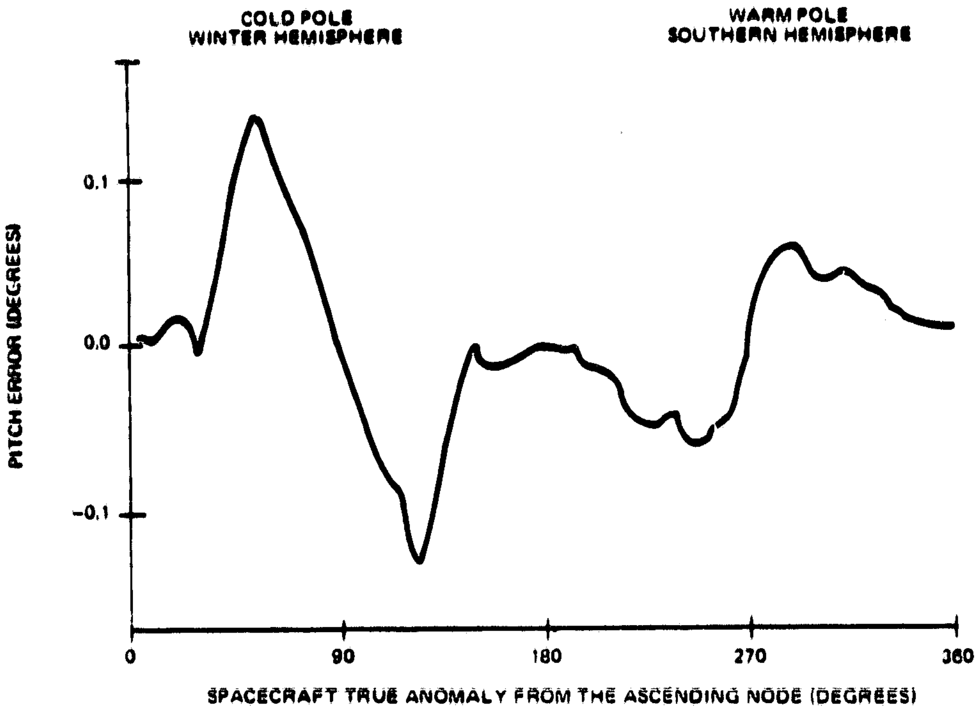

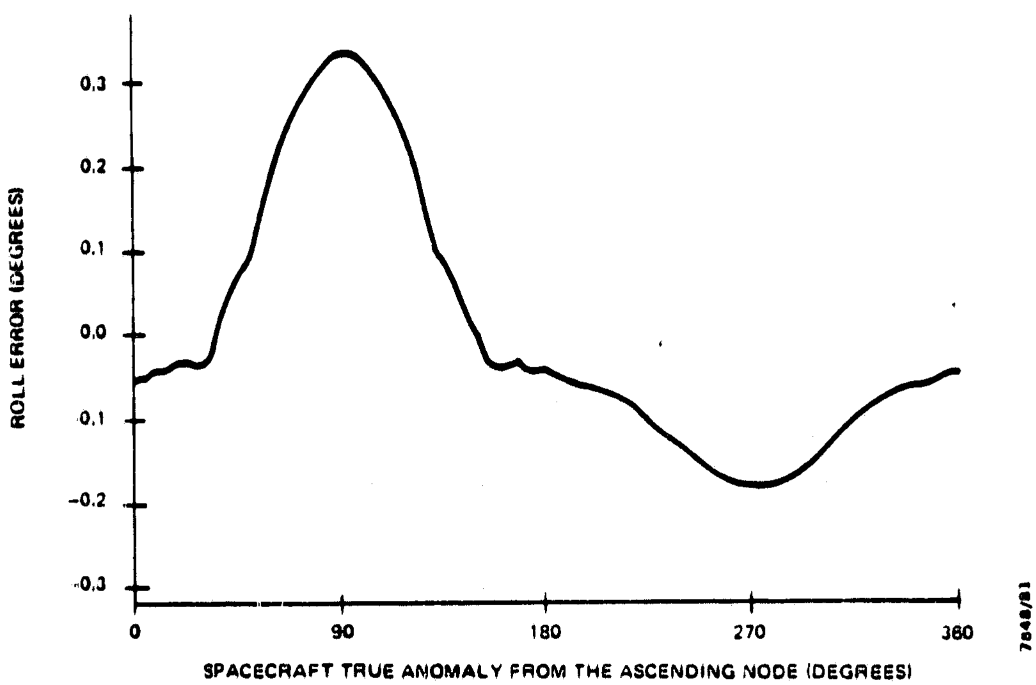

Figure 3-1 Magsat Systematic Horizon Radiance Corrections for January at 350-Kilometer Altitude (Reference 5)

radiance effects modeling methods. Both the Magsat and Seasat postlaunch sensor evaluations (References 5 and 6) pointed to errors in systematic horizon radiance modeling as a likely source of systematic error.

Any orbit frequency residual errors found from the Landsat-D data evaluation can probably be attributed to errors in the horizon radiance modeling, unless the scanner temperature is found to vary at orbit frequency with similar functional forms causing the temperature dependent pitch or roll bias to be indistinguishable from the horizon radiance modeling errors.

3.1.3 Calibration Adjustments

Error sources that have a dependence on specific variables will be considered as calibration adjustments. Two important calibration adjustments are discussed here.

3.1.3.1 Temperature Dependence

It is possible that the Landsat-D conical scanner measurements may show some dependence on either the sensor assembly temperature, or bolometer temperature or both. The sensor assembly temperature may affect the sensor electronics response and the scanner spin rate, and the bolometer temperature may affect the preamplifier gains. Since temperature data is available in the telemetry this dependence can be determined if a range of temperatures is observed in the flight data.

3.1.3.2 Earth Width or Phase Dependence

This error can result from errors in the slope or curvature of the scanner output voltage calibrations. This dependence can also be parameterized as a dependence on the spacecraft pitch and roll angles. On Landsat-D this dependence is unlikely to be detected because the attitude is not expected to have any significant variation from the nominal constant pitch and roll angles.

3.1.4 <u>Random Error Sources</u>

Noise from the sensor electronics is of high frequency and can easily be filtered out in data processing.

The lower frequency noises due to local radiance variations on the Earth, or cold clouds, are more difficult to handle. Since cold clouds have been found to be an important error source for past mission IR scanners, it will be important to see how much they impact the Landsat-D conical scanner performance which is designed to be less sensitive to cold clouds.

3.2 QUALITATIVE DATA REVIEW

Data plots in appropriate formats are a crucial tool for successful data evaluation, especially in the area of error analysis. This section discusses the parameters to be plotted, the data plot formats, the plot options appropriate for the Landsat-D conical scanner data evaluation, and how those plots may be utilized to analyze errors. Examples are provided from previous IR scanner evaluation efforts to illustrate the plot requirements.

A generalized plot package approach is recommended so that it will provide plots of any of the necessary data elements in order to demonstrate the correlations between the elements. The Calcomp plotter will be used to provide the high resolution plots needed for the evaluation effort.

3.2.1 Parameters to be Plotted

The main items of interest are the observed data, the predicted data based on the reference attitude, and the residual differences between them plotted as a function of time. Figure 3-2 shows a sample plot of these data items. Specific parameters of which these data items

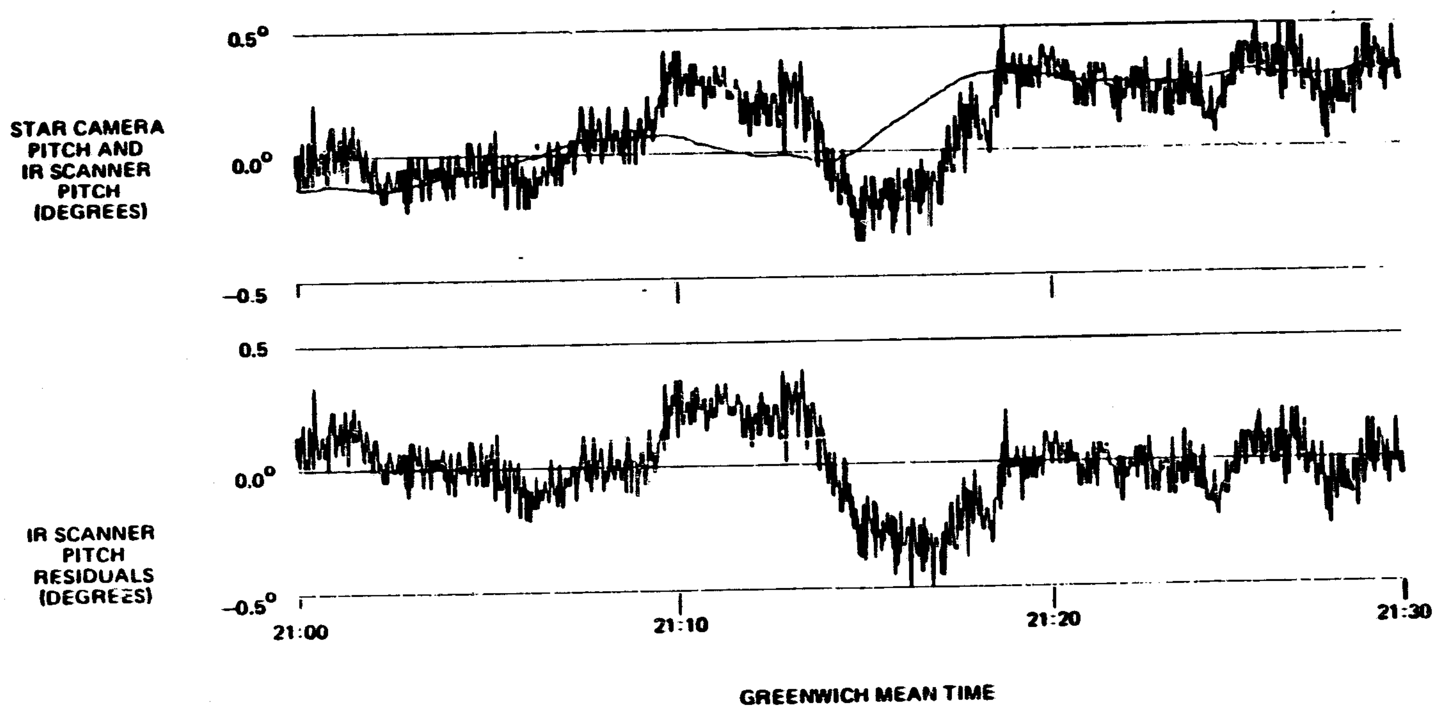

Figure 3-2 IR Sensor and Star Camera Pitch Data from Magsat on November 8, 1979 (Reference 5)

need to be plotted are discussed in the following. A summary of these parameters are given in Table 2-2.

The measurements from each scanner are the Earth width and phase angles, Ω and Φ. These measurements may also be provided in units of telemetry counts or scanner output voltages. These alternate units, which may be represented by a rescaling of the y-axis on the Ω, Φ plots, are not generally useful. The scanner measurements can also be converted by a linear transformation to approximate pitch and roll angle measurements which do not include adjustments for the effects of Earth oblateness and systematic horizon radiance variations and nonlinearities in their relationship with Ω and Φ. This approximate pitch and roll, p_o, r_o, is the one which is obtained for the conical scanners for use onboard Landsat-D by the analog controller and OBC. It will be included as an option to plot these pitch and roll measurements.

The Earth width and phase, Ω and Φ, measurements can also be parameterized somewhat differently as Earth-in triggering angles and Earth-out triggering angles, ϕ_{IN} and ϕ_{OUT}. They are the rotation angles of the scan cone when the Earth edges are detected. These angles are given by

$$\phi_{IN} = \Phi - \Omega/2$$
$$\phi_{OUT} = \Phi + \Omega/2 \qquad (3\text{-}1)$$

This alternate parameterization of the measurements is sometimes useful because it shows the measurement errors on each horizon crossing separately. Another useful representation of the horizon crossing measurements is as triggering heights, the apparent height of the sensor line of sight above the Earth surface when it registers the Earth CO_2 radiance edge. The computation of the Earth-in and Earth-out triggering heights, h_{IN} and h_{OUT}, involves more than just reparameterization of the measurements, since knowledge of the spacecraft attitude is required. Let Ω_p and Φ_p be the predicted Earth width and phase based on the OBC attitude and a nominal triggering height h_{NOM}, then

$$h_{IN} = h_{NOM} + \left(\frac{\partial(\Omega/2)}{\partial R}\right)^{-1} (-\phi_{IN} + \Phi_p - \Omega /2)$$
$$h_{OUT} = h_{NOM} + \left(\frac{\partial(\Omega/2)}{\partial R}\right)^{-1} (\phi_{OUT} - \dot{\Phi}_p - \Omega /2) \qquad (3\text{-}2)$$

where $\partial(\Omega/2)/\partial R$, the partial derivative of the half Earth width with respect to Earth radius, is given in Reference 1. These parameterizations of the measurements are useful for the analysis of cold cloud effects.

The scanner assembly temperature and the bolometer temperature are recieved from telemetry and will be plotted to examine the temperature variations. Also the OBC reference attitude pitch, roll, and yaw will be made available for plotting to examine the attitude variations.

It is useful to have an indicator of the spacecraft orbit position on the plots. An effective way to do this is to plot the spacecraft subsatellite latitude in parallel with the other plots. The spacecraft altitude can also be included as a plot option to show the orbit apogee and perigee positions.

3.2.2 Plot Options

Some flexibility in the plotting capability is essential. Clear plots of the data as a function of time are required for visual examination of the data characteristics. Marks of the time axis should be in even minute or ten minute intervals to provide an easy to read scale. The x and y axis scales must be adjustable, so that the plots can be set up to best show the data features. Varying time scales on the plots are useful to bring out features at different frequencies.

For example, it is best to plot several orbits of data in a fairly compact space in order to bring out orbit frequency effects.

It is useful to stack plots at orbit periods in order to demonstrate recurring orbit position dependent features. Figure 3-3 shows sample plots of this type.

Several plotted variables are required to be shown along the same time axis scale. This is an important feature for showing graphically any correlations between the events shown on the graphs. An example is given in Figure 3-4 of how the graphs can show a correlation in a way that is easy for the user to study. In this example, nutation of the Magsat spacecraft following a control torque is related to oscillations in the roll residuals that are just above the noise level in the IR data. Plots of subsatellite latitude and spacecraft altitude, alongside other plots, can be used to mark the orbit positions on the plots.

In addition to showing variables vs. time, another useful plotting option is the plotting of one variable against another to show the correlations. The variables that may be plotted this way to show particular correlations are discussed in Section 4.3.

ORIGINAL PAGE IS
OF POOR QUALITY

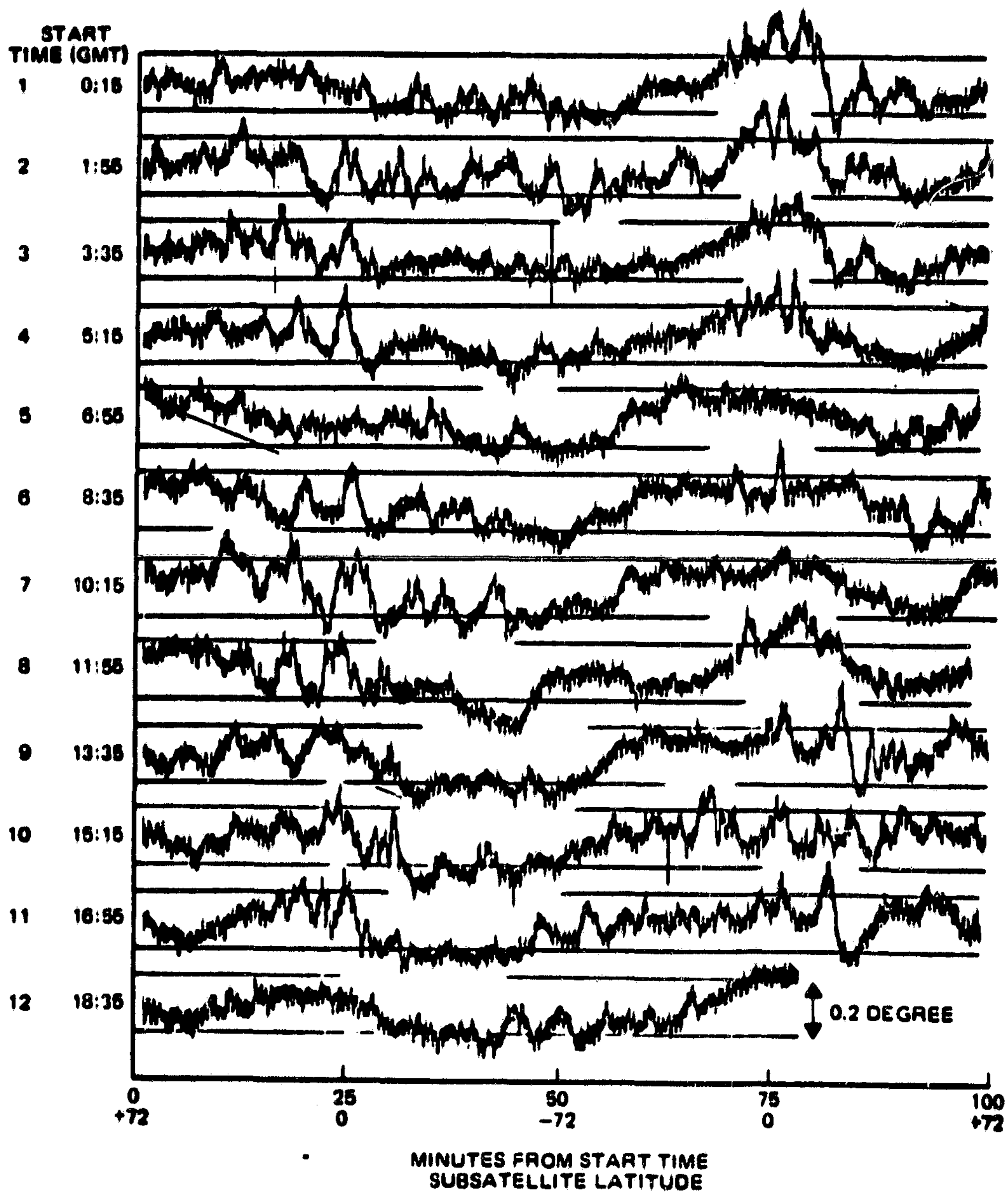

Figure 3-3 Seasat Roll Telemetry for 12 Orbits on October 2, 1978 Illustrating Cold Cloud Anomalies at the North and South Equator Crossings (Reference 6)

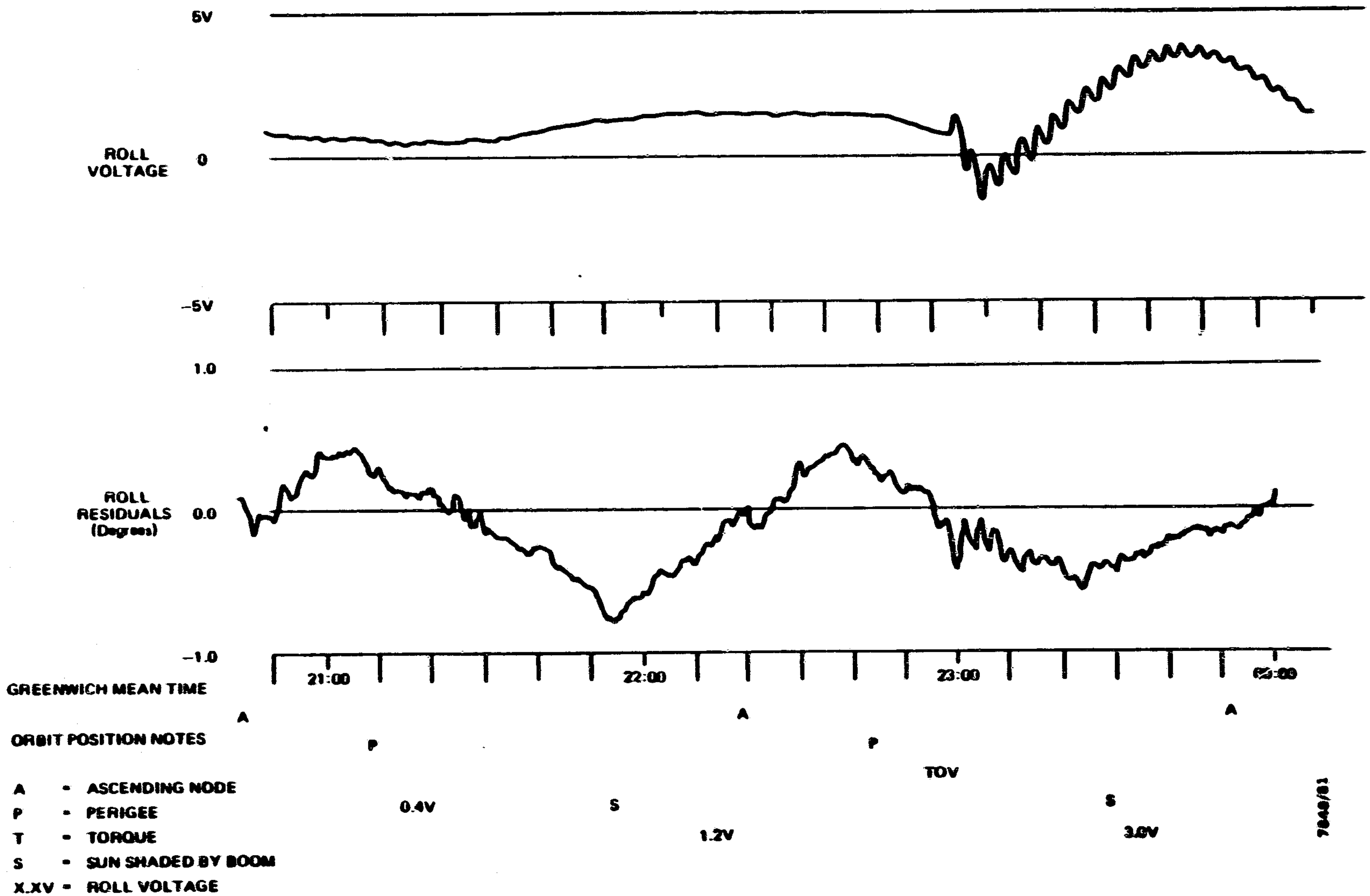

Figure 3-4 Magsat Roll Voltage and Roll Residual for November 9, 1979 (Reference 5)

3.2.3 Noise and Data Volume Reduction

It is sometimes necessary to reduce the noise and data volume in the data plots. This is particularly important when long data spans are plotted. N-point averaging, a simple but effective method of noise reduction, is recommended as an option in the data plotter. N-point averaging acts as a simple low-pass filter to remove the higher frequency components in the noise. Sample N-point averaging is shown in Figure 3-5.

3.2.4 Plot Formats and Review

Experimentation with the plots will be done to find good formats for displaying various features in the data. A standard format will be selected to display all the long data spans which are received. Particular formats may be chosen to show special features, such as the effects of cold clouds.

All available data will be plotted and reviewed closely to identify any unexpected features or anomolies in the measurements. The parameters which will be plotted for all available data spans will include the residual errors in the measurements (this is the main item of interest), and the bolometer and scanner temperatures

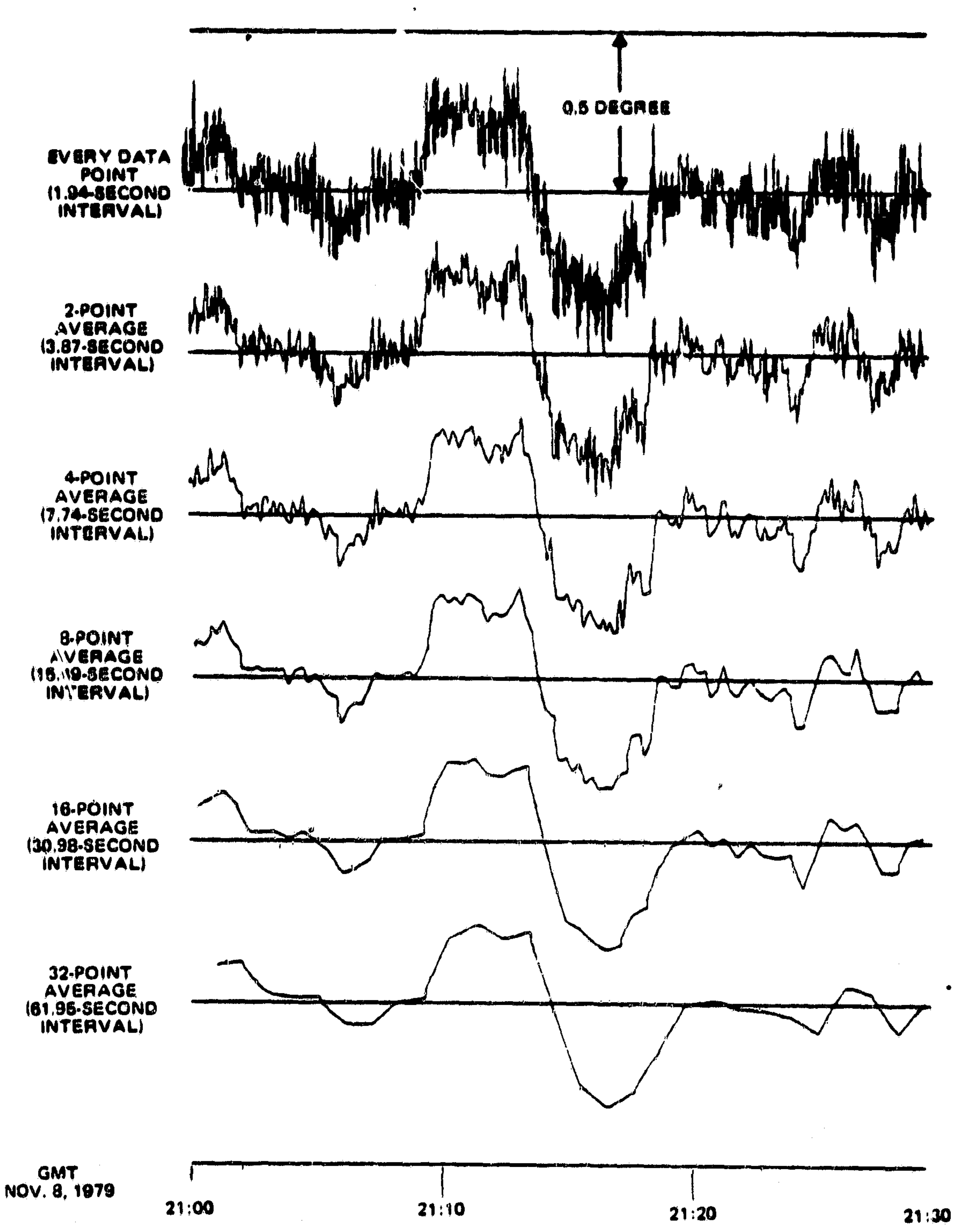

Figure 3-5 Effect of n-point Averaging on Magsat IR Scanner Pitch Measurement Errors

and reference attitudes (to check for any unusual variations). Other parameters will be plotted if analysis of the residuals indicates that some particular correlations should be investigated.

SECTION 4 - INFLIGHT SENSOR CALIBRATION AND PERFORMANCE EVALUATION

This section presents the procedures and techniques to be used in the inflight sensor calibration and performance evaluation for the Landsat-D conical scanner. Sensor calibration activities involve the determination of sensor modeling parameters to best explain the sensor measurement residuals due to systematic error sources. This is presented in Sections 4.1 to 4.4. The evaluation of sensor performance with regard to random error sources such as the effects of cold clouds is given in Section 4.5.

4.1 GENERAL MODEL ADJUSTMENT PROCEDURES

The goal of any sensor bias determination or calibration effort is the adjustment of sensor model parameters to explain the actual systematic variations in the sensor measurements. Automated bias determination procedures usually adjust the model parameters to minimize the root-mean-square (RMS) residual errors. Complex bias determination systems can have several model parameters adjusted simultaneously. Development of such systems is complex because they usually involve the computation of the partial derivatives of the observations with respect to all the model parameters. However in the case of bias determination or inflight calibration for the Landsat-D conical scanners, a complex automated bias determination software system will not be necessary, because bias determination can be accomplished with the following model adjustment procedures.

This procedure involves a detailed measurement predictor, which includes modeling of various error sources as described in Section 2.3, and a residual statistics and data fitting utility. The analytical considerations for this utility is given in Section 4.4. The most likely errors, namely the constant biases in the measurements, can be determined directly from the mean residual error. In fact, this approach determines the constant bias just as effectively as a least squares fitting procedure. In general, an optimal fit of any model parameter can be made by varying the parameter over several runs of the predictor to find the value that minimizes the RMS residual error. However this procedure can become tedious if many runs of the predictor become necessary. Therefore, for the biases that do not have constant effects on the measurements, two simple additional data analysis tools are recommended.

One is a low order polynomial fit routine to determine the relationship among observed variables. This allows the selection of calibration curve parameters. For example a temperature dependance or a roll angle dependence of the Earth width measurement errors can be determined. The slope or curvature of the observed relationship would indicate how to adjust the model parameters to optimally fit the data.

Another tool is a finite Fourier series fit routine. This would be particularly useful for identifying the orbital frequency effects in the data due to systematic errors such as seasonal horizon radiance variations.

Again, the fit parameters would dictate how to adjust the model parameters.

The identification of error sources for systematic residuals is important. However, when many of the systematic errors contribute to the same effects on the sensor measurements, they can hardly be distinguished from each other. It is important to note that for the case of Landsat-D, some of the correlated error sources may be separated by comparing the measurements obtained from the two conical scanners. Due to the different mounting geometrics and sensor scan path locations of the two scanners as shown in Figures 1-5 and 1-6, the effect on sensor measurements caused by the same error source are sometimes different for the two sensors. Some systematic errors may cause an effect on one sensor measurements but not on the other. This is shown in Table 3-1.

For example, all of the near orbital frequency errors (category 2 errors) give very little effect on the roll measurement of sensor 1 while both the pitch and roll measurements of sensor 2 are effected. Also, by comparing the constant pitch/roll errors of sensor 1 with those of sensor 2, errors due to pitch/roll offset biases may be distinguished from those due to Earth width/phase errors. Thus, it is always advantageous to compare data from two sensors to help in identifying the error sources in sensor bias determination.

4.2 CONSTANT BIASES

For missions like Landsat-D with a circular orbit and near zero-pitch-roll-yaw nominal attitude, most of the possible modeled bias parameters have nearly constant effects on the sensor measurements. As shown in Table 3-1, an Earth width bias, an Earth angular radius bias, a horizon triggering height bias, a scan cone angle bias, a scanner tilt misalignment or E voltage offsets will all make the Earth width larger or smaller at the nominal scan geometry. Likewise, a reference pulse time delay, a scanner twist misalignment, and a H voltage bias all have the same effect in changing the Earth phase measurement. In this situation, one bias parameter is adjusted which effectively compensates for the sum effect of all the correlated bias parameters.

The constant biases which will be adjusted for the Conical Scanners can be Earth width and phase biases. The equivalent biases in the other correlated parameters can easily be computed.

The mean residual error indicates the constant bias which will minimize the RMS error. The term "constant bias" in this context thus means the average bias over the data span.

Some care must be taken to look for slow variations in the mean residual errors. If there is little variation in the general character of the residual errors over time, this constant bias determined will be about the same no matter what data span is used. However because some likely non-constant error effects will vary at orbit frequency, it will be wise to use an integer multiple of a full orbit period for optimal determination of the "constant bias" independently of the particular data span. A "constant bias" can be determined for each day that data is available, and the consistency of these daily "constant biases" will indicate the overall stability of the biases over longer time scales.

4.3 CALIBRATION CURVES

The non-constant measurement bias effects can be studied with calibration curves. The calibration curve formulation for biases assumes that the measurement errors show some dependence on another variable. It is generally the case that this dependence is nearly linear, or possibly having a slight quadratic curvature. Thus a low-order polynomial fit routine is recommended for identifying calibration curve measurement corrections. The other recommended option for fitting the dependence between variables will be a selected set of sinusoidal waves, using the finite Fourier series fit. This option will be especially useful for adjusting the horizon radiance effects model.

The calibration adjustment approach is purposely made general, so that if unexpected relations appear in the flight data between the various observed and predicted parameters, these relationships can be analyzed without software modifications.

Two particular error sources to be calibrated with these fitting procedures are described below.

4.3.1 Temperature Effects

There is the possibility that the scanner measurements will be influenced by the scanner assembly temperature or bolometer temperature. A first order polynomial will probably be adequate to fit any observed temperature dependence. The observability of this dependence requires finding data with some temperature variation, and information is not now available on how these temperatures will vary in flight. This dependence will only be determined if adequate temperature variation is encountered in the available data spans.

4.3.2 Horizon Radiance Model Adjustments

Systematic horizon radiance variations will cause a variation in horizon triggering height as a function of horizon crossing latitude. The triggering heights will be lower in the winter hemisphere and higher in the summer hemisphere. In the middle seasons, the triggering height variations cause an oblateness like effect.

The estimate of these effects will be made by using the sensor optics and electronics simulator (SOES) in combination with an Earth radiance model as shown in Figure 2-4. The triggering height variation predicted by this model will be fit by a finite Fourier series function whose exact terms will be selected based on the predicted functional form of the dependence (optionally, polynomial terms may be added). The likely form of the dependence will be

$$h(\ell) = h_o + a_1 \sin(\ell) + a_2 \cos(2\ell) + a_3 (3\ell) + a_4 \cos(4\ell) \tag{4-1}$$

where ℓ is the horizon crossing latitude.

A dependence will be determined separately for the Earth-in and Earth-out horizon crossings.

Using the flight data, the residual differences in the observed and predicted triggering heights will be examined. Based on the functional form of the observed residual errors, an adjustment will be calculated for some of the finite Fourier series fit terms, by fitting the residual errors.

4.3.3 Other Calibration Relationships

A brief mention is made here of some other calibration relations which will probably not be applicable to Landsat-D because of the mission attitude/orbit geometry. These calibrations, which have been done on other missions, would be to show dependence of the measurement residuals on the following items

1) Spacecraft Pitch Angle

2) Spacecraft Roll Angle

3) Spacecraft Altitude

The Landsat-D nominal attitude/orbit will show very little variation in these parameters, therefore determination of residual dependence on these parameters will be difficult. However, because the calibration software will be designed in a general way, the calibration could be done if there is enough variation in these parameters to indicate a dependence.

4.4 ANALYTICAL CONSIDERATIONS

4.4.1 Basic Statistics

It is important to make a statistical evaluation of the fit between the predicted and observed data. The mean and root-mean-square (RMS) or standard deviation of the residual errors are the main statistics of interest. The mean residual errors give good indications of the constant biases needed to optimize the fit. The standard deviation shows the variations in the residuals about the mean.

The specific definitions of these statistics are

$$r_{mean} = \frac{1}{N} \sum_{i=1}^{N} r_i \quad \text{(mean residual)} \tag{4-2}$$

$$r_{rms} = \sqrt{\frac{1}{N} \sum_{i=1}^{N} r_i^2} \quad \text{(RMS residual)} \tag{4-3}$$

$$\sigma_r = \sqrt{\frac{1}{N-1} \sum_{i=1}^{N} (r_i - r_{mean})^2} \quad \text{(standard deviation estimate)}$$

$$= \sqrt{\frac{N}{N-1} (r_{rms}^2 - r_{mean}^2)} \tag{4-4}$$

where r_i is the observed minus predicted residual errors for the N observations in the data span.

4.4.2 Polynomial and Fourier Series Fits

The finite order polynomial and Fourier series fits will be discussed together because they are obtained by the same method. The n^{th} order polynomial relationship between two variables is given by

$$y = \sum_{k=0}^{n} p_k x^k \tag{4-5}$$

where p_k is the k^{th} order coefficient.

The finite Fourier series fit is given by

$$y = \sum_{k=0}^{n} \left[a_k \sin(kx/P) + b_k \cos(kx/P)\right] \tag{4-6}$$

where a_k, b_k are the k^{th} order Fourier coefficents and P is a known period for the function.

Both of the above formulas share the characteristic that they are linear in the coefficients. We may write the following general representation for equations with linear coefficients.

$$y = c_1 f_1(x) + c_2 f_2(x) + \dots + c_n f_n(x) \tag{4-7}$$

$$= \sum_{k=1}^{n} c_k f_k(x)$$

The least square fit to data provides the optimal estimate for model parameters based on the assumption that the observation noise is random with a Guassian distribution (Reference 7). The least squares fit minimizes the sum of the squares of the residual observation errors:

$$\chi^2 = \sum_i (y_i - f(x_i))^2/\sigma_i^2 \tag{4-8}$$

where f is presumed dependence of y on x and (x_i, y_i) are the coincident observations of x and y. This sum may be weighted by a different uncertainty σ_i in each observation, although often all the observations are assumed to have the same uncertainty.

Thus the quantity which must be minimized in a least squares fit of Equation (4-7) is given by

$$\chi^2 = \sum_i \left[\frac{1}{\sigma_i} \left(y_i - c_1 f_1(x_i) - c_2 f_2(x_i) - \ldots - c_n f_n(x_i) \right) \right]^2 \tag{4-9}$$

χ^2 is minimized when its partial derivative with respect to each of the coefficients is zero, i.e., when

$$\frac{\partial \chi^2}{\partial c_1} = -2\sum_i \left[\frac{f_1(x_i)}{\sigma_i^2} \left(y_i - c_1 f_1(x_i) - c_2 f_2(x_i) - \ldots - c_n f_n(x_i) \right) \right] = 0$$

$$\frac{\partial \chi^2}{\partial c_2} = -2\sum_i \left[\frac{f_2(x_i)}{\sigma_i^2} \left(y_i - c_1 f_1(x_i) - c_2 f_2(x_i) - \ldots - c_n f_n(x_i) \right) \right] = 0 \qquad (4\text{-}10)$$

$$\vdots$$

$$\frac{\partial \chi^2}{\partial c_n} = -2\sum_i \left[\frac{f_n(x_i)}{\sigma_i^2} \left(y_i - c_1 f_1(x_i) - c_2 f_2(x_i) - \ldots - c_n f_n(x_i) \right) \right] = 0$$

The above equations can be rewritten as the following to more explicitly show the relationship among the coefficents

$$\sum_i f_1(x_i) y_i = c_1 \sum_i f_1(x_i)^2 + c_2 \sum_i f_1(x_i) f_2(x_i) + \ldots + c_n \sum_i f_1(x_i) f_n(x_i)$$

$$\sum_i f_2(x_i) y_i = c_1 \sum_i f_2(x_i) f_1(x_i) + c_2 \sum_i f_2(x_i)^2 + \ldots + c_n \sum_i f_2(x_i) f_n(x_i) \qquad (4\text{-}11)$$

$$\vdots \qquad\qquad \vdots$$

$$\sum_i f_n(x_i) y_i = c_1 \sum_i f_n(x_i) f_1(x_i) + c_2 \sum_i f_n(x_i) f_2(x_i) + \ldots + c_n \sum_i f_n(x_i)^2$$

where the σ_i^2 in the denominator of each summation has been omitted for simplicity.

Equation (4-11) represents n simultaneous equations in the n unknown coefficients. These equations can be solved by standard methods.

In matrix representation we may write equation (4-11) as

$$\vec{Y} = [M]\,\vec{C} \tag{4-12}$$

where

$$Y_k = \sum_i \frac{f_k(x_i)y_i}{\sigma_i^2} \tag{4-12a}$$

$$M_{j,k} = \sum_i \frac{f_j(x_i)f_k(x_i)}{\sigma_i^2} \tag{4-12b}$$

The solution to Equation (4-12) is given by

$$\vec{C} = [M]^{-1}\,\vec{Y} \tag{4-13}$$

The matrix [M] can be inverted as long as the functions $f_k(x)$ are linearly independent, and at least n independent observations are made. In fact, the polynomial and finite Fourier series equations are linearly independent.

The particular terms in a given finite Fourier series or polynomial fit between variables can be selected based on an analytical understanding of the expected relationship between the variables. Then the summations in Equations (4-12a) and (4-12b) can be computed over the observations and the appropriate coefficients can be solved for.

4.5 COLD CLOUD EFFECTS EVALUATION

Detailed examination of Ithaco Scanwheel* IR scanner measurements from previous missions has shown that cold clouds on the horizon are the most significant source of measurement noise (Reference 8). This cold cloud noise is of low frequency compared to the data rate, with excursions in the measurements lasting on the order of minutes as the horizon moves in and out of cloudy regions on the Earth. Sample plots of the excursions in Seasat scanner measurements that are attributed to cold clouds are shown in Figure 4-1.

Cold clouds are high altitude clouds usually associated with frontal systems or thunderstorms. Clouds block the infrared radiation from below and emit thermal radiation at the temperature of the cloud tops. The reduced thermal radiation from the cold clouds impacts the IR scanner horizon measurements.

Differences in the design of the Conical Scanner compared to the Scanwheel were made to reduce the sensitivity to cold clouds and weather conditions. The differences include a slower scan rate, and a different horizon locator logic (see Figure 1-4). However, some

* Scanwheel is a registered Trademark of Ithaco Inc.

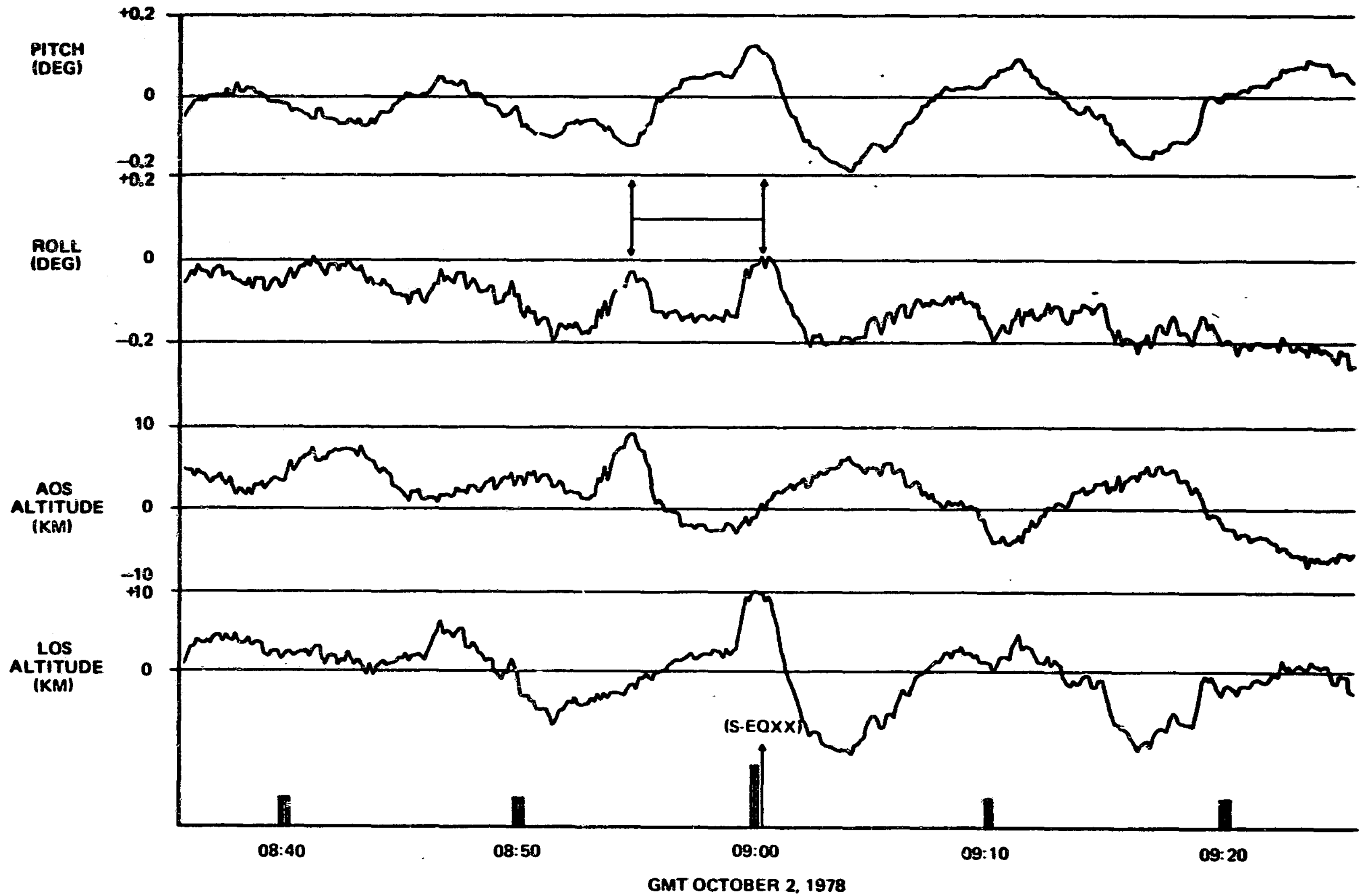

Figure 4-1 Seasat Scanwheel Pitch and Roll Telemetry near the Southbound Equator Crossing (S-EQXX) on October 2, 1978, Illustrating the Effects of a Cloud at 150 degrees West Longitude, 15 degrees North Latitude. The relative Earth-in (AOS) and Earth-out (LOS) Altitudes were computed assuming a nominal spacecraft attitude (Reference 6).

sensitivity to cold clouds on the horizon may remain, and it will be of interest to examine this sensitivity and compare it with the previous IR scanners.

4.5.1 Cold Cloud Effects Identification

The following items are required for the empirical evaluation of the effects of cold clouds on the horizon scanner measurements.

- Plots of several hours of data so that good examples of flight over isolated cold clouds can be located.
- A printout of the horizon positions viewed by the scanners as a funct.on of time.
- A utility program for plotting the scan paths on the Earth.
- Infrared photographs of the Earth showing the cloud cover for the data span and places of interest.

These items are discussed in more detail in the following.

Plots of Long Data Spans

For any given data span, the clouds may be scattered so that it is hard to see clearly the impact on the measurements. However, when long data spans are reviewed, many good clear examples of the effects of isolated cold clouds can be found. The flight over an isolated cloud shows clearly the effect of the cloud against the nominal, clear sky measurements.

When plotting the data for the examination of cold cloud effects it is useful to represent the measurements as Earth-in and Earth-out triggering angles, so the effects on each horizon crossing can be seen separately. These plots may be parameterized as Earth-in and Earth-out triggering heights as a convenient indicator of the horizon detection effects.

Also it is useful to stack plots of the various horizon measurements over the same time scale, so that the cloud crossings effects can be identified by their simultaneous signatures in some of the measurements, as to be discussed in Section 4.5.2.

<u>Horizon Position Printout</u>

The horizon positions of the Earth viewed by the scanner can be computed given the OBC attitude or estimated from the nominal spacecraft attitude. Since the scanner field of view actually sweeps over a range of horizon positions, a representative point must be selected. For example this could be the center of the field-of-view at the time it is one degree inside the Earth edge. It is the cloudiness or clear conditions approximately at this point, just inside the Earth edge, that affects the measurements. However, on the Seasat Mission, it was the cloudiness of a threshold adjust region five to eleven degrees of scan rotation inside the Earth edge that affected the measurements.

The exact scan position to be used as the horizon sighting position indicator can be a variable in the software, so that adjustments can be made based on the observed cloud effects using the more detailed scan description below.

Scan Path Plots

A more complete description of the scanner field-of-view intersection with the Earth surface can be provided by a scan path plotting utility. Such a utility was developed for the Seasat and Magsat cold cloud effects analysis. This utility program plots the scan path on a projection of the Earth grid. Thus the scan path plots generated could be overlaid on GOES Earth infrared images to give clear graphical correlation of the scan path intersections with clouds on the Earth. A sample plot from this overlay process is given in Figure 4-2 for the Seasat mission.

Infrared Meteorological Photographs

Infrared photographs of the Earth showing the cloud cover for the times and places of interest are needed to confirm that errors in the scanner measurements are due to the cold clouds.

These photographs not only provide picturial indications of the cloud positions, but they also provide an indication of the cloud top temperatures from the imagery gray scales. These photographs can be obtained from the Environmental Data Service of the National Oceanograhic and Atmospheric Administration.

The photographs are available in several formats. Full Earth Disk Images, like the sample in Figure 4-2 are taken every 30 minutes by GOES meteorological satelites in synchronous orbit. The GOES east satellite is positioned over 75° west longitude above South America. The GOES west satellite is positioned at 135° west longitude over the Pacific Ocean.

ORIGINAL PAGE
BLACK AND WHITE PHOTOGRAPH

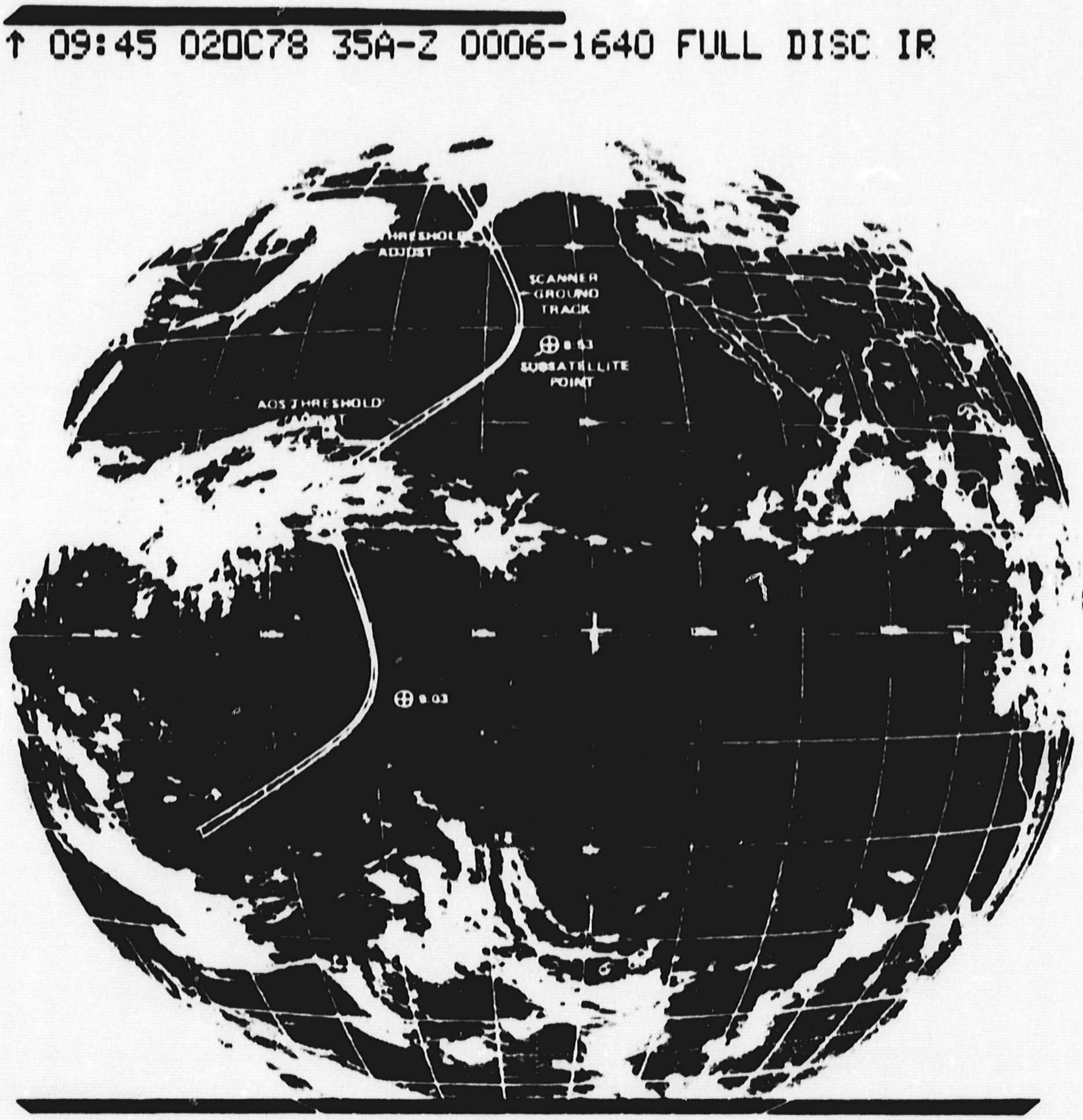

Figure 4-2 Seasat IR Scanner Ground Tracks at 8:53 and 9:02 GMT on October 1, 1978 Overlaid on GOES Western Satellite Earth Infrared Image (Reference 6 , photo from NOAA).

For coverage of the polar regions and the other side of the globe, one can obtain mapped mozaic photographs, generated from the low altitude polor orbiting meteorological satellite data. A sample of this type of photo is shown in Figure 4-3 from NOAA-2 satellite data. The polar orbiting meteorological satellites are in Sun synchronous orbits with one side of the orbit in daylight and one in darkness. Two mozaics are accumulated for each day, one for the day side of the orbit and one for the night side. Thus the time resolution of the available data is not as fine as for the synchonous orbit imaging satellites. However this coverage is adequate to show the general meteorological features, which do not have much change over one day.

Correlation Procedures

The correlation of measurement effects with cold cloud crossings is a straightforward procedure given the tools discussed above. The empirical identification of cold cloud effects can proceed in two directions. Cloud crossings can be identified in the photographs, and then the data can be examined for excursions at the corresponding times. Alternatively, excursions in the sensor measurements can be identified and it can be checked whether these excursions correspond to cold

ORIGINAL PAGE
BLACK AND WHITE PHOTOGRAPH

Figure 4-3 Northern Hemisphere Mapped Mozaic Infrared Photograph from NOAA-2 Satellite Data on Night Side of Orbit.

cloud crossings. Both procedures are useful. For the latter approach, the following analysis is useful.

4.5.2 Landsat-D Cold Cloud Signature

When examining the data plots for the effects of cold clouds, it is helpful to look for correlated excursions in the measurements, which are referred to as cold cloud signatures. These correlated excursions result from the scanner mounting geometry which causes Earth-in and Earth-out horizon crossings to pass over the same place on the Earth at different times.

The nominal ground track of the Landsat-D Conical Scanner relative to the spacecraft flight path is shown in Figure 1-6. It can be seen from this figure that both the right scanner horizon crossings and the tail scanner Earth-out horizon crossing will pass over nearly the same positions on the Earth.

Based on the nominal orbit altitude, the true anomaly rate for the satellite will be 3.64 degrees per minute (or .275 minutes per degree). Therefore after the Scanner 2 Earth-out crossing views a cloud, about 10 minutes transpire before the Scanner 1 Earth-out crossing and the Scanner 2 Earth-in crossing veiw the same cloud.

The Landsat-D conical scanner cold cloud signature is shown schematically in Figure 4-4. This figure shows the effects of clouds on the various IR scanner measurements, as a function of time. For this discussion, it is assumed that the presence of a cloud on the horizon will lower the horizon triggering height. The theoretical prediction of the effect of a cloud on the horizon detection is discussed in the next subsection.

The first part of Figure 4-4 shows the effects of an isolated cloud on the right side of the ground track (cloud no. 1). The Scanner 2 Earth-out crossing first encounters the cloud. Then about nine minutes later the Scanner 1 Earth-out crossing encounters the cloud, followed about a minute after that by the Scanner 2 Earth-in crossing. The remainder of the figure shows the effects of some more complex patterns of clouds (clouds no. 2 to 6). Note that when both the Earth-in and Earth-out horizons are cloud covered, the effect on the E voltages (scanner 1 pitch and scanner 2 roll) is doubled while the effect on the H voltages (scaner 1 roll and scanner 2 pitch) cancels out.

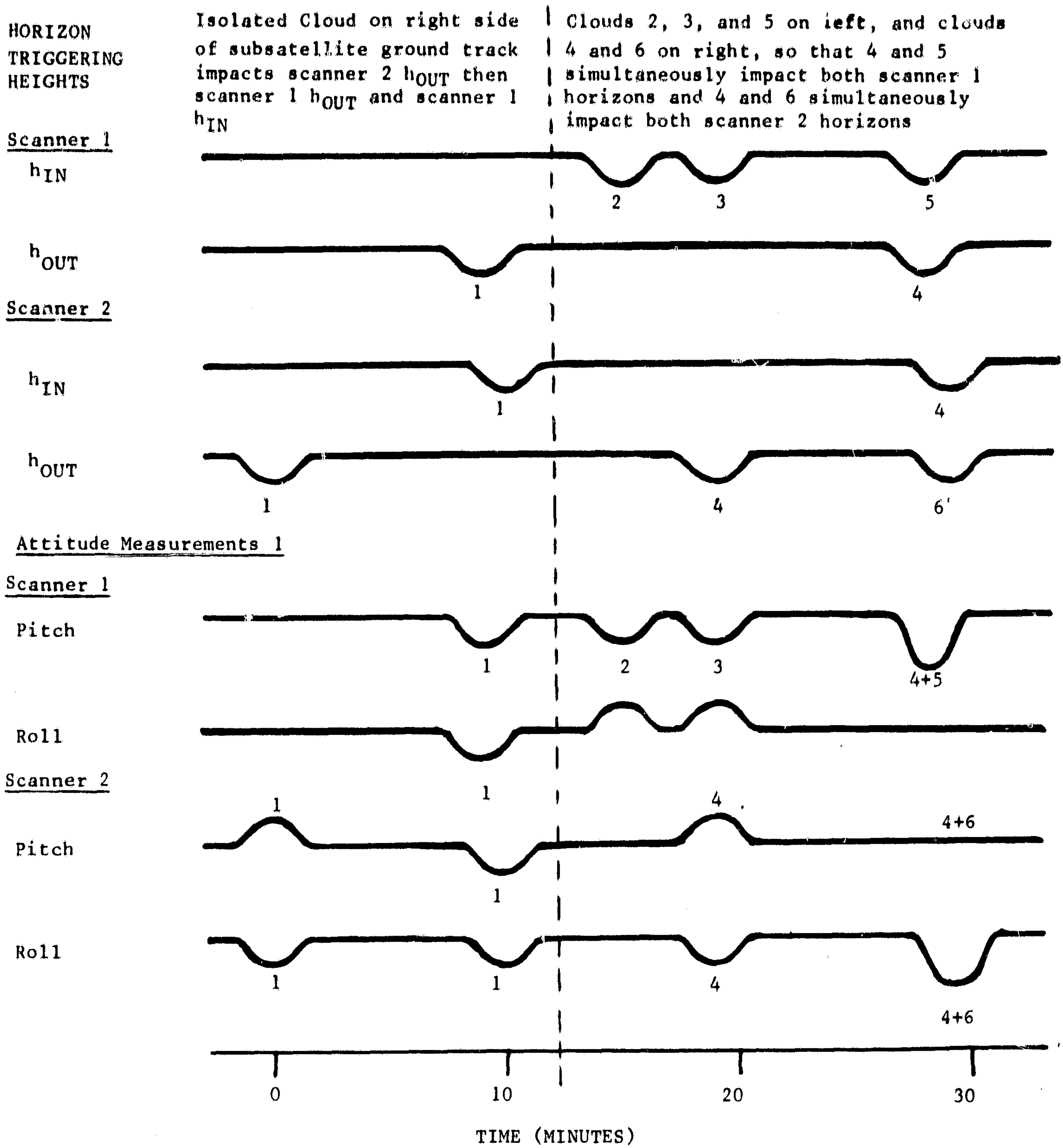

Figure 4-4 Landsat-D Cold Cloud Signatures

4.5.3 Theoretical Estimate of Effects

The estimate of the effects of cold clouds on the sensor measurements requires modeling of the sensor optics and electronics.

The sensor optics and electronics simulator which will be developed to analyze seasonal systematic radiance effects, can also be used as an analytical tool to predict the effects of cold clouds on the sensor measurements. To do this, the simulator can be run with radiance profiles representing cold cloud conditions to compare with the nominal, clear sky radiance profiles.

SECTION 5 - DATA SPAN REQUIREMENTS

This section discusses the data spans which are required to meet the various evaluation goals.

An adequate data base is essential for proper evaluation of the inflight IR scanner performance. Long data spans are important for several reasons which will be discussed below. Ideally it would be useful to have all the mission data reviewed in the evaluation process, but usually this is not practical. This section reviews the data spans which are required for a good evaluation effort, but more data could be included if it does not generate data access problems and a data processing burden.

C-2

5.1 DATA AVAILABILITY

Detailed information is not available at this time on the Landsat-D data acquisition schedule. However, there are two spacecraft tape recorders, designed to hold about 4 hours of data. This corresponds to over 2 orbits of data per tape recorder. If the tape recorders are used alternately, continuous data coverage could be provided. The following discussion assumes that fairly continuous coverage is available, and states the data spans desirable for analysis.

5.2 DATA SPAN REQUIRED FOR DETERMINATION OF VARIOUS EFFECTS

Since orbit frequency systematic effects are of special interest in the data evaluation it will be important to have data spans of several full orbits. In order to examine the longitude dependance on radiance variations a 24 hour data span would prove optimal.

Also, it will not be adequate to calibrate the data by taking just one long data span. Since systematic radiance effects change with the seasons, a detailed evaluation of these effects requires multi-orbit (preferably 24 hours) data spans at various seasons. A group of observations taken monthly would provide an adequate indication of the seasonal variations.

It is necessary to provide information on the long term stability of the sensor calibration results so that gradually changed biases can be identified. Monthly evaluation of multi-orbit (perferably 24 hours) data spans would also serve to meet this need.

The possibility of calibrating the scanners for the temperature dependance of the measurments depends on the availability of data at a significant range of temperatures. Information is not available at this time on the expected variations in the scanner and electronics temperatures. Therefore, when the data becomes available it will be scanned to look for the periods of widest temperature variation to use for the determination of temperature dependant effects.

REFERENCES

1. S. Bilanow, L. Chen, I. Kulikov, "Landsat-D Conical Scanner Mathematical Modeling," General Software Corporation, GSC-TR8202, February 1982.

2. A. Das, "The On-Orbit Attitude Determination and Control System for the Landsat-D Spacecraft," AIAA 20th Aerospace Sciences Meeting, Orlando, Florida, AIAA-82-0310, January 1982.

3. R. Talipsky, "Landsat-D Data Format Control Book Volume II (Telemetry)," General Electric, SVS10123, July 31, 1981.

4. F. Kneizys, et.al., "Atmoshperic Transmittance/Radiance Computer Code LOWTRAN5," Air Force Geophysics Laboratory (OPI), AFGL-TR-80-0067, ERP No. 697, February 21, 1980.

5. S. Bilanow, "Magsat Infrared Horizon Scanner Data Evaluation Report," Computer Sciences Corporation, CSC/TM-81/6043, March 1981.

6. C. Manders, et.al, "Seasat-1 Postlaunch Attitude Analysis," Computer Sciences Corporation, CSC/TR-79/6008, June 1979.

7. P.R. Bevington, "Data Reduction and Error Analysis for the Physical Sciences," McGraw Hill Book Company, New York, 1969.

8. S. Bilanow, M. Phenneger, "The Response of the Seasat and Magsat Infrared Horizon Scanners to Cold Clouds," Fifth Annual Flight Mechanics/Estimation Theory Symposium," NASA CP 2152, October 1980.